
SURFACE TENSION DRIVEN FABRICATION OF THREE-DIMENSIONAL MICROSTRUCTURES

Author: Janarthanan Sundaram

Date: 28 august 2010

Versie: 3.0



M.Sc. Thesis University of Twente

Group: Transducer Science and Technology Group

Committee: Prof.Dr.ir. M. Elwenspoek, Dr.ir. L. Abelmann, Dr.ir. N.R. Tas, Dr.ir. J.W. van Honschoten, Ing J.W. Berenschot, Dr. J. Snoeijer.

Reference:

Period: Nov. 2009 – august 2010

TABLE OF CONTENT

| | | |
|-------|---|----|
| 1 | Introduction..... | 3 |
| 1.1 | motivation | 3 |
| 1.2 | Outline of this project..... | 4 |
| 2 | Theory | 5 |
| 2.1 | Capillary forces | 5 |
| 2.1.1 | Folding with capillary forces..... | 6 |
| 2.1.2 | Effects of different contact angles | 12 |
| 2.1.3 | Varying the structural dimension..... | 14 |
| 3 | Folding templates..... | 15 |
| 3.1 | Method | 15 |
| 3.1.1 | Design of the templates | 15 |
| 3.1.2 | Cleanroom processes | 17 |
| 3.1.3 | Experimental setup | 18 |
| 3.2 | Results | 19 |
| 3.2.1 | First results folding structures with more the 2 flaps. | 19 |
| 3.2.2 | Results of folding of prism..... | 19 |
| 4 | Folding with different contact angle | 22 |
| 4.1 | method | 22 |
| 4.1.1 | white light measurement using lateral scanning interferometry | 22 |
| 4.2 | Results | 24 |
| 5 | Varying design of the prisms | 25 |
| 5.1 | Problem definition..... | 25 |
| 5.1.1 | Torsion in folding..... | 25 |
| 5.1.2 | Folding without symmetry | 26 |
| 5.1.3 | Varying contact area | 28 |
| 5.1.4 | Lifting objects out of the plane | 28 |
| 5.2 | Results | 29 |
| 5.2.1 | Torsion in folding..... | 30 |
| 5.2.2 | Folding without symmetry | 30 |
| 5.2.3 | Varying contact area | 32 |
| 5.2.4 | Lifting objects out of the plane | 34 |
| 6 | Conclusion | 36 |
| 6.1 | Recommendation | 37 |
| 7 | Bibliography | 38 |
| 8 | Appendix – process documents | 39 |

1 INTRODUCTION

1.1 MOTIVATION

The invention of the transistor led to a revolution which made possible that almost every household owns a computer. Even more, everyone can have a computer in his pocket nowadays, the contemporary mobile phone has more capacity than a supercomputer of the 70's. This all was possible not only by the invention of the transistor, but also by the invention of the whole process that was needed to make millions of transistors on a single silicon chip. This technology is now mature and is being used to develop new types of technologies.

A process technology is Micro Electro Mechanical Systems, also called MEMS. As the name already implies this technology creates small mechanical systems which interact electrically. Figure 1 gives an impression of the scale of these mechanical devices. These systems are used in sensors and can also be found in contemporary mobile phones, which react to movement, or have a compass function. These structures are made with the same technology as computer chips, all the components lay planar on the surface. Also this can be seen in the figure. This planar disposition of the structures limits the possibilities of this technology. The possibilities will be dramatically increased if there was a way to create MEMS devices that stood up from the surface.

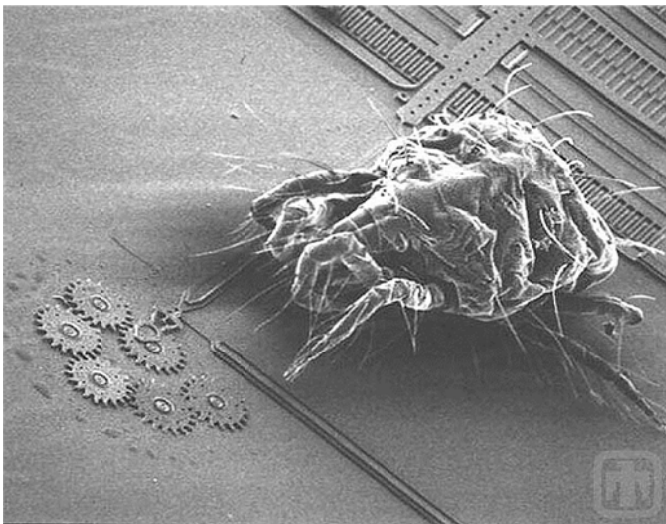


FIGURE 1 SCANNING ELECTRON MICROSCOPE IMAGE OF A SPIDER MITE ON A POLYSILICON MEMS GEAR-TRAIN. SPIDER MITES RANGE IN SIZE FROM 0.5 MM TO 1 MM. (1)

In this report we will discuss a method to create three dimensional structures by folding flat pieces of silicon nitride like the ancient Japanese technique called origami. The structures are of course on a micro scale, so the folding method has to be as such that a small structure can be folded. The method we use is the capillary force of water drops to fold the structures. This is because capillary forces become dominant at smaller scales.

We all know the small insects that walk on the water, this is possible due the capillary force also called the surface tension of the water. This same force can be used to fold structures. One single drop is enough to fold a an silicon nitride template into a structure like a pyramid.

1.2 OUTLINE OF THIS PROJECT

In this project we are going to fold a template made in silicon nitride using standard IC technology and fold this into three dimensional structures. Folding will be done by using the capillary forces of water drops. At first we will determine the theoretical forces working on these structures when a drop of water is placed on them, and assess whether these structures can be made to fold. And if they fold, will these structures stay folded? We will determine the folding rate and how different surface parameters will influence this rate. The structures and theoretical model are already created and determined.

The folding of the structures led to new effects which we will investigate experimentally. Effects that posed new questions were that of the structures stayed folded after folding and that the structures kept folding seamlessly every single time. We will look at the stiffness of hinges, the geometry, the manner in which we dispense water and the surface characteristics of the structures. Getting a clear picture of the forces that play role.

All these experiments will give enough data to give an understanding on the folding of silicon nitride structures. In addition to all this we will try to lift the logo of the university out of the plane, and try dispense a drop of water through a channel, instead of dispensing water off hollow fiber used in the experiments

We will discuss the created model of folding in chapter 2. In this chapter the theory behind capillary folding and how this force can be harnessed for folding structures. The setup and the method how we did these experiments are elaborated in chapter 3.1. Different experiments are spread out over different chapters and have sub results. This is the chronological order in which the experiments were done. Results of the Simple folding experiments can be found in chapter 3.2, experiments with variation of the structure parameters can be found in chapters 4.2 and 5.2. This is followed by an overall conclusion and recommendations.

2 THEORY

2.1 CAPILLARY FORCES

The force we use to fold structures is the same force that can be seen in really narrow tubes, also called capillaries. When these tubes are placed in a bath of water, the water will tend to flow into the tube upwards regardless of gravity. This phenomenon is used by plants to get water with nutrients from the soil to everywhere in their system. But the same force can be witnessed as surface tension, this phenomena is used by water striders to walk on water. Same force is responsible for sticky hair when coming out of the shower or that wet glasses stick to flat surfaces. A drop of water with a radius of 1 cm can hold two glass plates together with a force of 10N, so hold a glass plate of 1 kg

This all can be explained by the fact that molecules in liquids want to be surrounded by other molecules from the same liquid. Molecules on the surface will have half less molecules surrounding them than other molecules in the fluid as illustrated in Figure 2. This is an unfavorable energy state. This is the reason that fluids adjust their shapes to minimize the exposed surface. The exposed surface is also called the liquid air interface. This minimization of the interface manifests in forming of droplets.

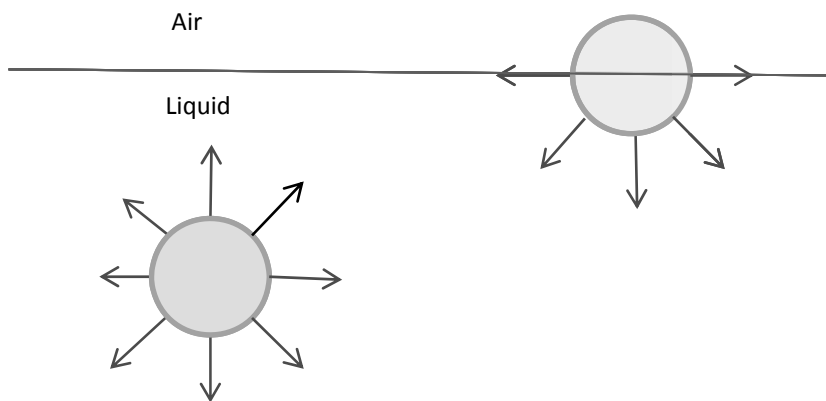


FIGURE 2 LIQUID AIR INTERFACE, TOP MOLECULE IS NOT HAPPY BECAUSE IT IS NOT SURROUNDED BY SAME KIND OF MOLECULES

Every liquid is specific how it reacts to the solid surfaces. This has a lot to do with surface tension. The interface where the liquid reacts to the solid is called to solid liquid interface, and how the liquid reacts to air is called liquid air interface. These interface forces depend on the liquid. A contact angle measurement of the liquid will give an angle to the shape of the droplet on a solid plane. This angle relates directly to the solid liquid interface factor. These forces become dominant when we scale down, and thus become favorable In this application. An example of this scaling is a small insect that can walk on water using surface tension, but an elephant cannot walk on water. Or if we would look at a straw with water we will see that the water stands higher against the inner wall of the straw, and if we look at a shoreline we will not see this effect. As shown in Figure 3.

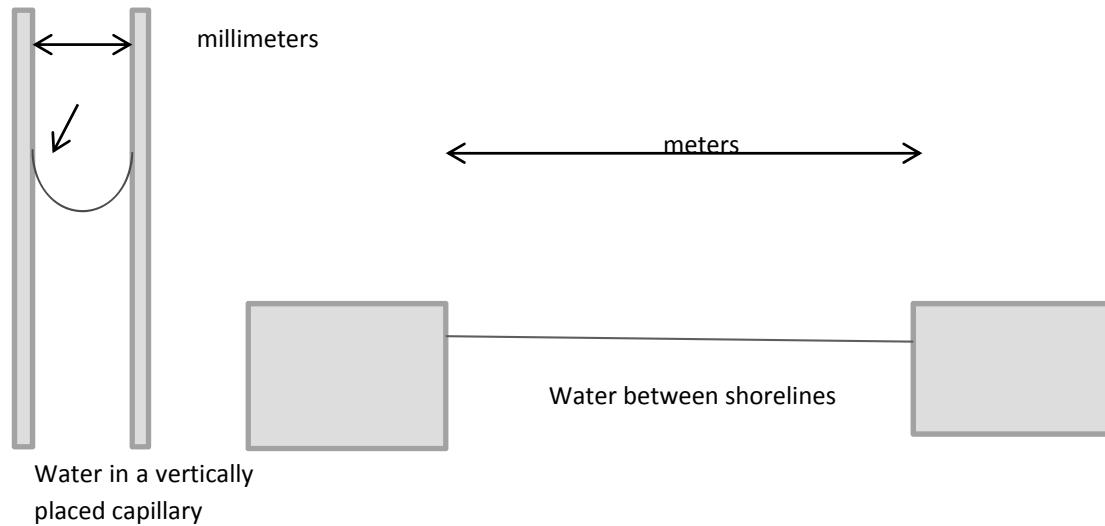


FIGURE 3 DIFFERENCE BETWEEN WATER IN A TUBE AND LARGE WATER BODIES. THERE IS A CLEAR EFFECT ON THE EDGE OF THE TUBE BUT THERE NONE ON THE EDGE OF A SHORELINE

When drop is placed on a surface the drop can form a thin film or become a drop. This depends on the surface and liquid characteristics. This is quantified by the contact angle θ_c .

When a drop tends to become a thin film on a surface we call this fully wetting. When considering water it will fully wet a SiN surface. This is the material our templates are made of. Other liquids will react differently to this surface and may form a droplet. In this case the contact angle of the drop with the surface can be measured by viewing the drop.

2.1.1 FOLDING WITH CAPILLARY FORCES

It was proven recently (2) that when a drop of water is put on a thin sheet of polymer, the polymer would spontaneously wrap. This is due to that the drop will try to minimize the water air interface, the capillary force will fold the polymer sheet as shown in Figure 4. As you can see in the figure the sheet of plastic is on a millimeter scale. After folding the water will totally evaporate. As already explained in the previous chapter this effect should become larger when we scale down to micrometers.

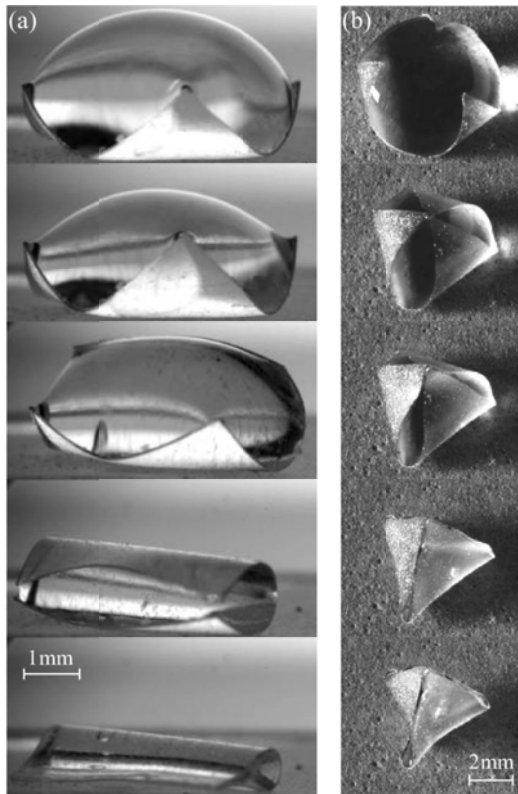


FIGURE 4 WRAPPING OF DROP OF WATER WITH SQUARE AND TRIANGULAR SHEETS OF PDMS (POLYDIMETHYLSILOXANE) EXAMPLE OF FOLDING ON A MILLIMETER SCALE.

There was a demonstration of assembling millimeter sized structures using capillary effects using molten solder. Placing solid solder on the hinges and melting the solder made the structures stand up from the plane (3). This was scaled down to scale of 100nm. Problem with this technique is that the solder will be left on the hinges. For folding it would be great if we could combine the scale of the last technique and the benefits of using water.

By using water on templates the TST group already folded various structures (4) with the use of water. As seen in Figure 5(a) to (d). The design of the templates are shown in Figure 5(a). These templates are designed for production by conventional lithographic processes, and therefore it is designed in planar manner. More about the production processes can be found in chapter 3.1. Folding the long structure results in a prism shaped object as shown in Figure 5(b). The top center template results in the shape as shown in Figure 5 (c) and the most right top template results in the cube as shown in Figure 5 (d). The black bar in these figures are all of the same size, namely 50 μ m.

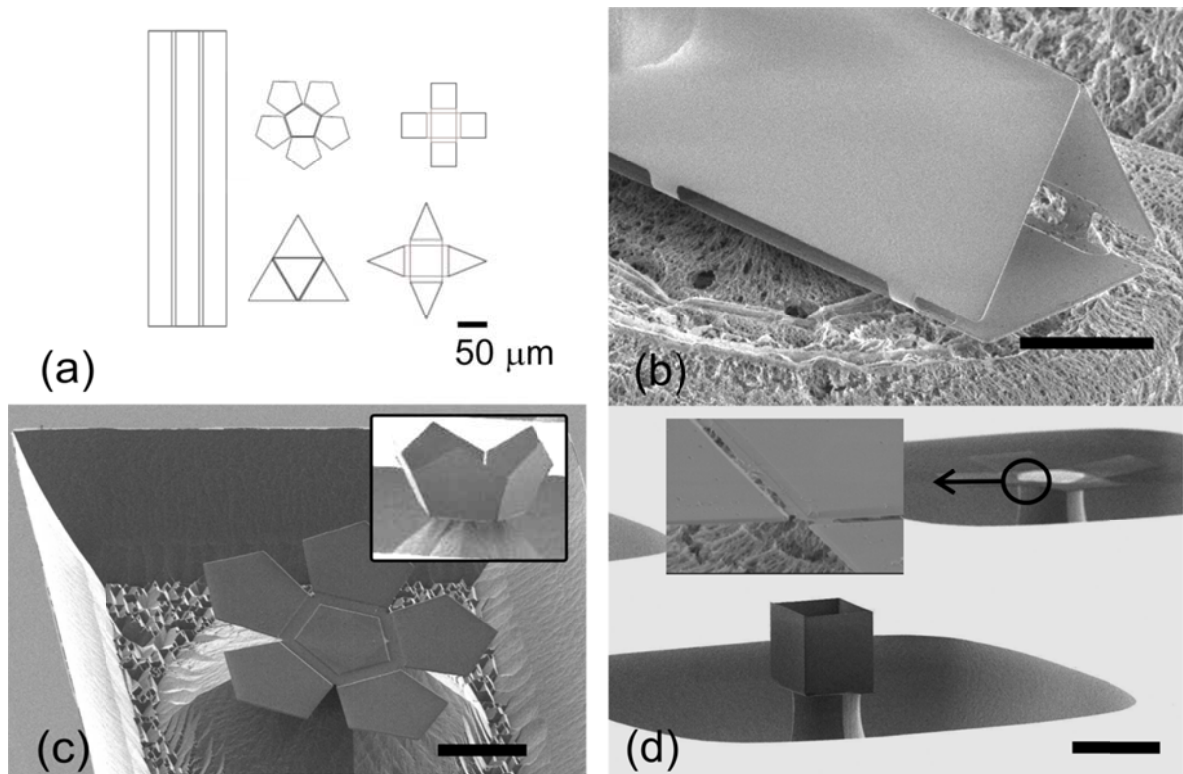


FIGURE 5 (A) DESIGN TEMPLATES (B) FOLDED PRISM (C) OPEN AND FOLDED HALF A DODECAEDER (D) FOLDED AND OPENED CUBE WITH ZOOM IN ON THE HINGES (D)

The prism structure is specially designed to verify the two dimensional theoretical model the group already made. Because a prism structure is much longer than that it is wide, we can neglect longitudinal dimension and just take the front view. By doing this simplification the variables we can distinguish are the angles of the flaps and the volume of water on the structure. A front view of the template of a prism is shown in Figure 6, in this figure the flaps are bent slightly. The hinge is depicted as a thinner line, l_0 is the length of the hinge and t is the thickness. Structures can behave in two manners, either the hinges are too stiff and the structure folds a little and then opens, or the hinges are loose enough so that the structure can fold completely. These two types of transitions are shown in figure 8 and Figure 9. In these figures the flaps are shown schematically making different angles and the water meniscus is shown as a thin line. The end result of the folding progression as shown in Figure 9 is shown in Figure 5 (b). An artist impression of the folded prism is shown in Figure 7.

We will make the following assumptions, the edges of the droplet is pinned down on the edges of the flap. The structure is fully wetting and the drop covers the whole surface of the structure. To form a model of the progression of folding we need to define the following dimensions as shown in Figure 10. This figure shows the model where we again take the front view of a prism to simplify the model. W is the width of the flaps, ϕ the angle that flaps make when folding. The curvature of the meniscus on the structure can be seen as a part of a circle. The angle of this piece of this circle is θ . Figure 6 shows the bending of a hinge, where l_0 is the length of the hinge, t is the thickness of the hinge; if we take l_0 as a part of a circle then R is the radius of this circle.

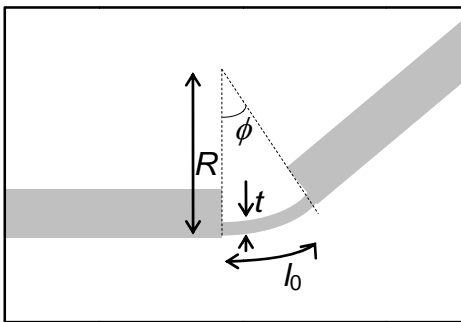
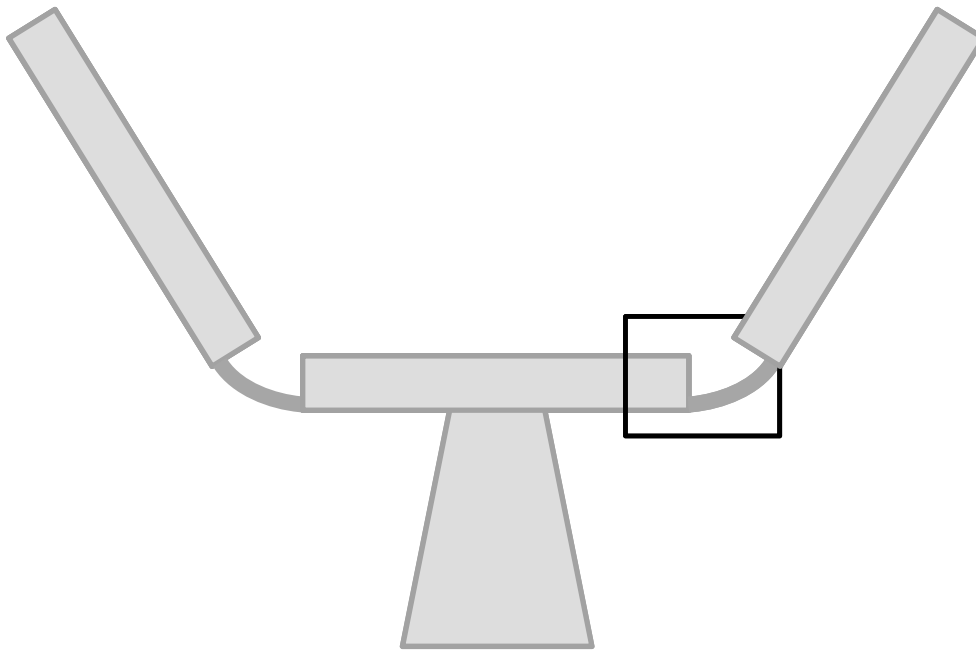


FIGURE 6 BENDING A THE HINGE, WHERE l_0 IS THE LENGTH OF THE HINGE, t THE THICKNESS AND ϕ THE ANGLE THAT THE HINGE MAKES

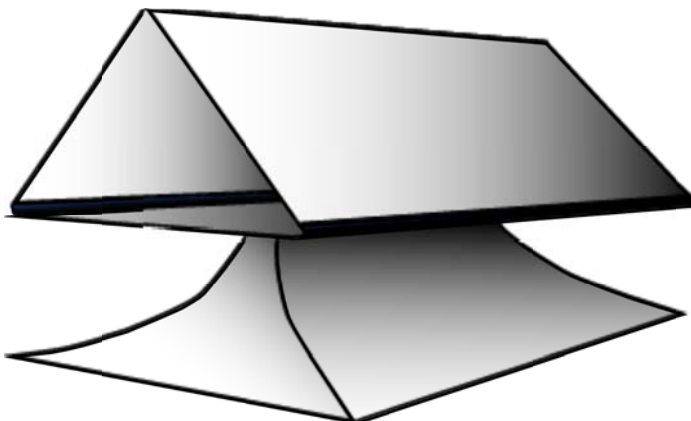


FIGURE 7 ARTISTS IMPRESSION OF A FOLDED PRISM

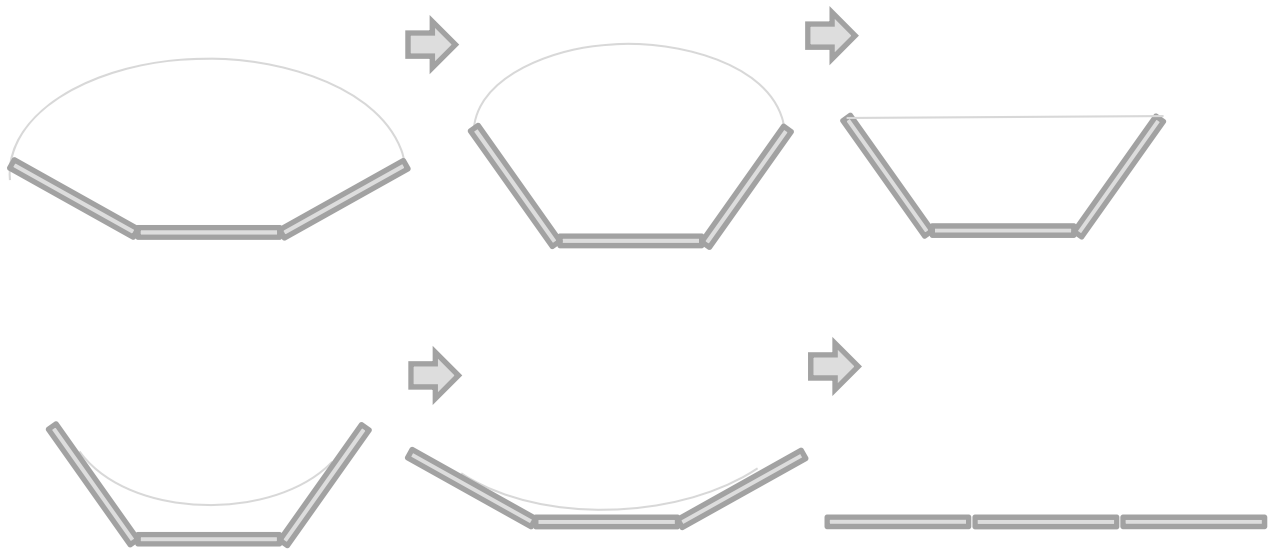


figure 8 schematic overview of the front view of a prism while Folding and opening progresses

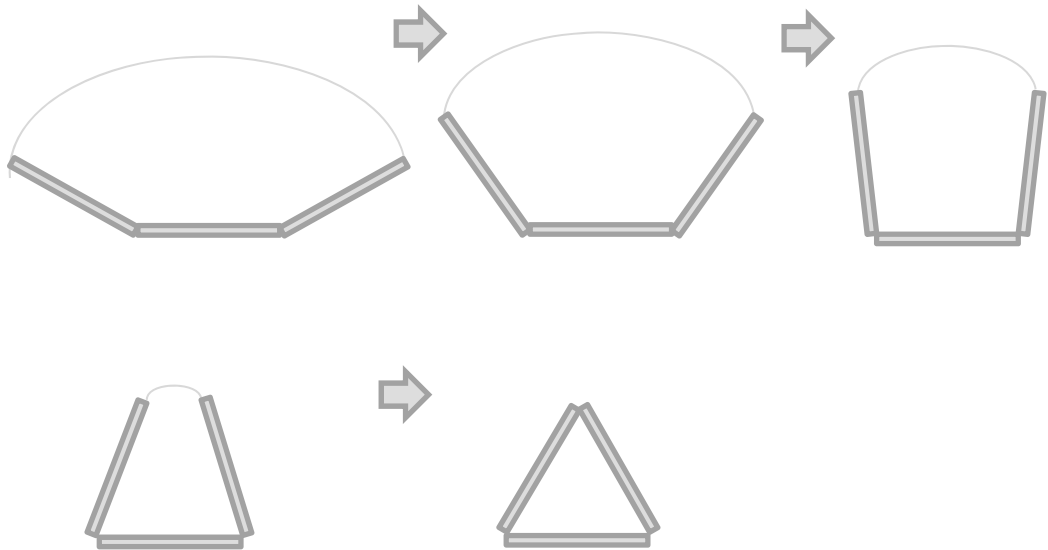


Figure 9 schematic overview of the front view of a prism while Folding progresses

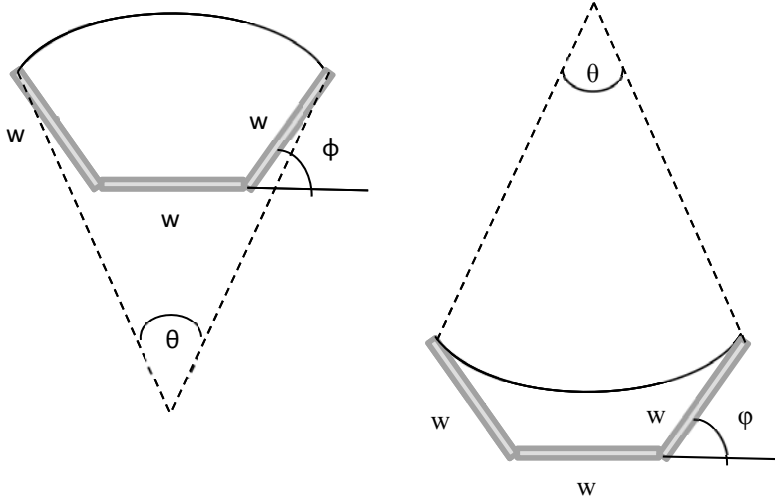


FIGURE 10 THE VARIABLES FOR THE MODEL, w IS THE WIDTH OF A FLAP, ϕ IS THE ANGLE THAT THE FLAP TAKES, WHEN CONSIDERING THE MENISCUS AS A PART OF A CIRCLE THEN θ IS THE ANGLE OF THE TIP OF THIS PART. RIGHT FIGURE SHOWS THE CONCAVE SHAPE OF THE MENISCUS WHEN ENOUGH WATER IS EVAPORATED AND THE STRUCTURE DID NOT FOLD COMPLETELY

A droplet placed on the surface will tend to minimize the liquid air interface and deform the structure by bending the flaps. The total energy of the system consists of the elastic energy in the hinges and the liquid-air interface of the droplet. The bending energy of a curved plate can be written as $\frac{B}{2R^2}$ and where $B = \frac{Et^3}{12(1-\nu^2)}$ is the bending stiffness. E is the Young's modulus and ν the Poisson's ratio. Bending the flaps over the angle ϕ results in a bending energy per unit length as: $\bar{U}_b = \theta \frac{\frac{1}{2}\phi^2 B}{l_0}$. The surface energy of the liquid air interface can be written as $U_\gamma = \frac{\gamma w \theta (\cos(\phi + \frac{1}{2}))}{\sin(\frac{\theta}{2})}$. If we normalize this per unit length: $\bar{U} = \theta \frac{\cos(\phi) + \frac{1}{2}}{\sin(\frac{\theta}{2})} + \beta \phi^2$

Where $\beta = \frac{B}{l_0 \gamma w}$ is the balance between mechanical bending forces and capillary forces. When taking the total volume and in our simplification the surface S as constant, the relation of the angles ϕ and θ can be found with: $\frac{\theta (\cos\phi + \frac{1}{2})^2}{2 \sin^2(\frac{\theta}{2})} - \frac{(\cos\phi + \frac{1}{2})^2}{\tan(\frac{\theta}{2})} + \sin\phi + \frac{1}{2} \sin(2\phi) = \sigma$ and $\sigma = \frac{S}{w^2}$ is the normalized cross section.

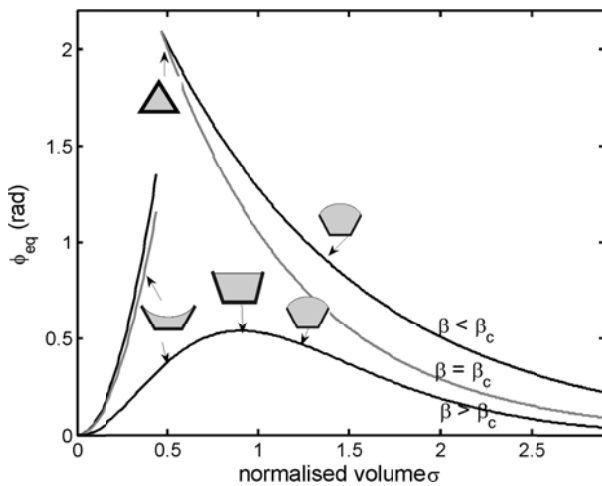


FIGURE 11 PHASE DIAGRAM OF THE EVOLUTION OF EQUILIBRIUM STATES AS FUNCTION OF VOLUME

If we minimize the energy \bar{U} in respect to ϕ resulting in an equilibrium angle of ϕ_{eq} . As we can see in Figure 11, how the equilibrium angle change depends on the stiffness parameter β . For a certain stiffness of the hinges

the flaps bend due to evaporation of the droplet to a certain angle and then open again after attaining the equilibrium angle ϕ_{eq} , this is shown in Figure 11 as the line where $\beta > \beta_c$. For a certain lesser stiffness the flaps fold completely into a prism. The ϕ_{eq} in this case is reached when completely folded. This is depicted as the line $\beta < \beta_c$. The stiffness β_c is the threshold stiffness value where we get the transition from folding and opening into folding completely. For angles ϕ_{eq} smaller then $\frac{2}{3}\pi$ the flaps will not close completely and will open again after reaching this angle. At the angle $\phi_{eq} = \frac{2}{3}\pi$ the flaps close completely this corresponds to $\sigma = \frac{1}{4}\sqrt{3}$. Reducing σ any further will result in a ϕ_{eq} not larger than 1.39 rad, leading to a discontinuous transition in the diagram. This means that the structure will abruptly reopen again.

In Figure 11 we see that for $\beta > \beta_c$ the interface shape transitions from a convex in to a concave shape. On the transition point the angle of the interface will be zero ($\theta = 0$), from this we can find β_c . \bar{U} has a minimum for $\phi_{eq} = \frac{2}{3}\pi$ and this results in $\beta_c = \frac{3}{4\pi}\sqrt{3}$. Note that there is a gap between after that $\phi_{eq} = \frac{2}{3}\pi$. According to this model after the gap the structure should fold open.

2.1.2 EFFECTS OF DIFFERENT CONTACT ANGLES

Previous experiments we used the fully wetting surfaces. This means that the contact angle of the water with the surface of the structures is pinned down at the edges and the angle that the water makes with the edge is totally dependent on the volume of water.

For not fully wetting surface the curvature of the meniscus is dependent on the contact angle this is shown in Figure 12. Looking at this figure one might observe that there is an dependency between θ and θ_c . This dependence is clearly illustrated in Figure 13. We can deduce from this figure that $\alpha = 180^\circ - 90^\circ - \phi - \frac{1}{2}\theta$ and $\alpha = 90^\circ - \theta_c$, this results in $\frac{1}{2}\theta = \theta_c - \phi$. Substituting this in the energy function formulated in the previous chapter will result in $\bar{U} = (\theta_c - \phi) \frac{\cos(\phi) + \frac{1}{2}}{\sin(\frac{\theta_c - \phi}{2})} + \beta\phi^2$. This means that now the energy is not dependent on θ but dependent on θ_c .

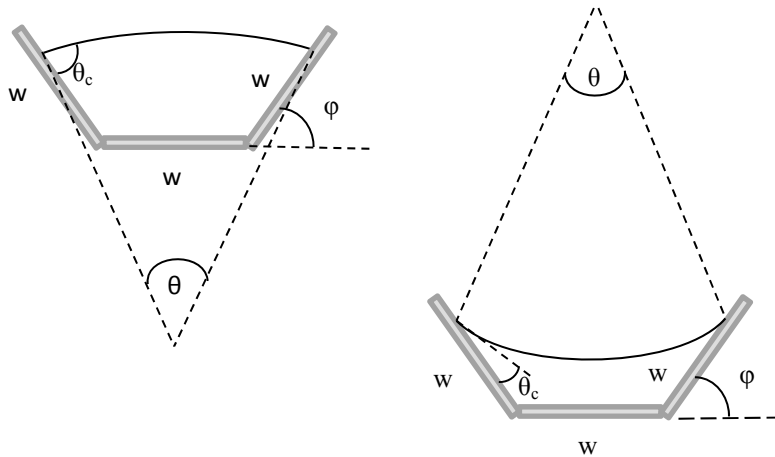


FIGURE 12 SCHEMATIC OVERVIEW OF THE MODEL AND VARIABLES WHEN THE LIQUID IS NOT FULLY WETTING . θ_c IS THE CONTACT ANGLE, w IS THE WIDTH OF A FLAP, ϕ IS THE ANGLE THAT THE FLAP TAKES, WHEN CONSIDERING THE MENISCUS AS A PART OF A CIRCLE THEN θ IS THE ANGLE OF THE TIP OF THIS PART. RIGHT FIGURE SHOWS THE CONCAVE SHAPE OF THE MENISCUS WHEN ENOUGH WATER IS EVAPORATED AND THE STRUCTURE DID NOT FOLD COMPLETELY.

It was already proven that folding structures are following the theoretical model, so to see the effect of the a fixed contact angle it is not necessary to perform all the angle measurements. We need to determine where the maximum point of the progression lies, the maximum equilibrium angle ϕ_{eq} , as shown in figure 14. We can then see how this maximum equilibrium angle changes for different contact angles θ_c . in Figure 15. As in the previous model the question arises whether the experimental results will follow this model.

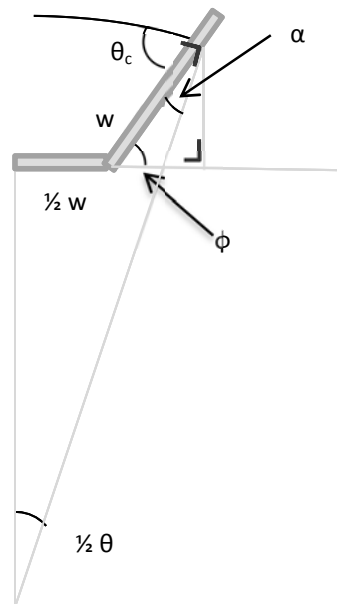


FIGURE 13 HOW CONTACT ANGLE IS RELATED TO θ

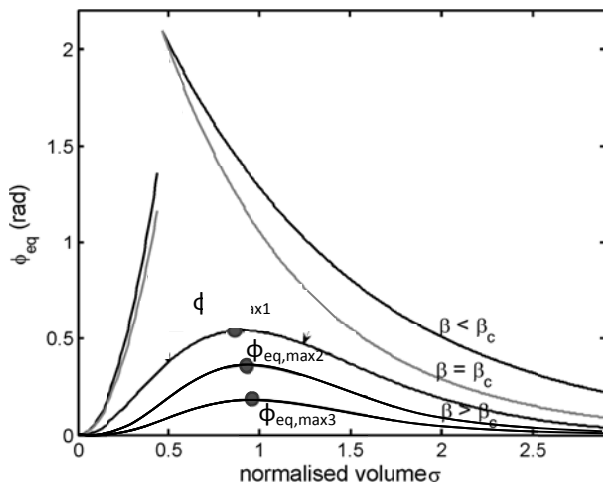


FIGURE 14 MAXIMUM EQUILIBRIUM ANGLES FOR DIFFERENT CONTACT ANGLES

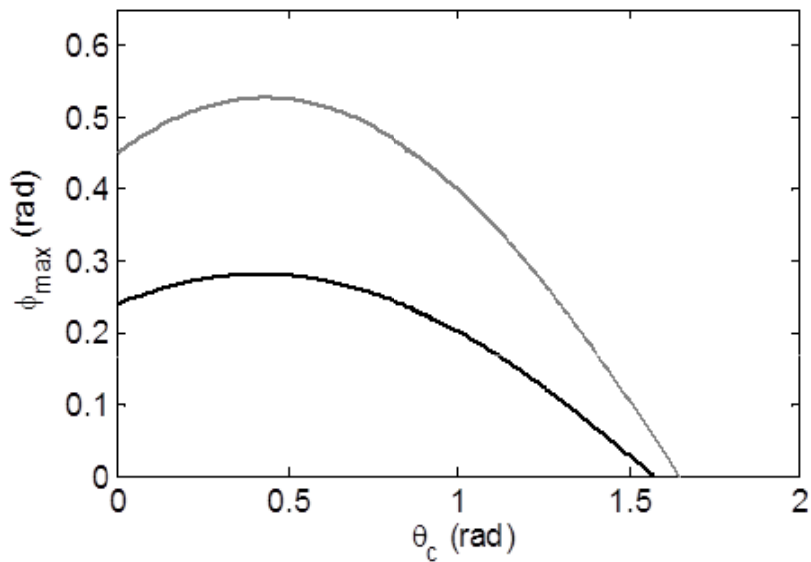


FIGURE 15 HOW THE MAXIMUM ANGLE CHANGES DUE TO THE CHANGE OF CONTACT ANGLE

2.1.3 VARYING THE STRUCTURAL DIMENSION

Experiments done reveal new phenomena which need to be examined more. The structures that fold stay folded. SEM picture show that there are some material on the edge of the fold. This might be the cause of the fact that structures stay folded. To get a better idea about the amount of force that is holding the flaps folded we need change the are over which the flaps are glued together.

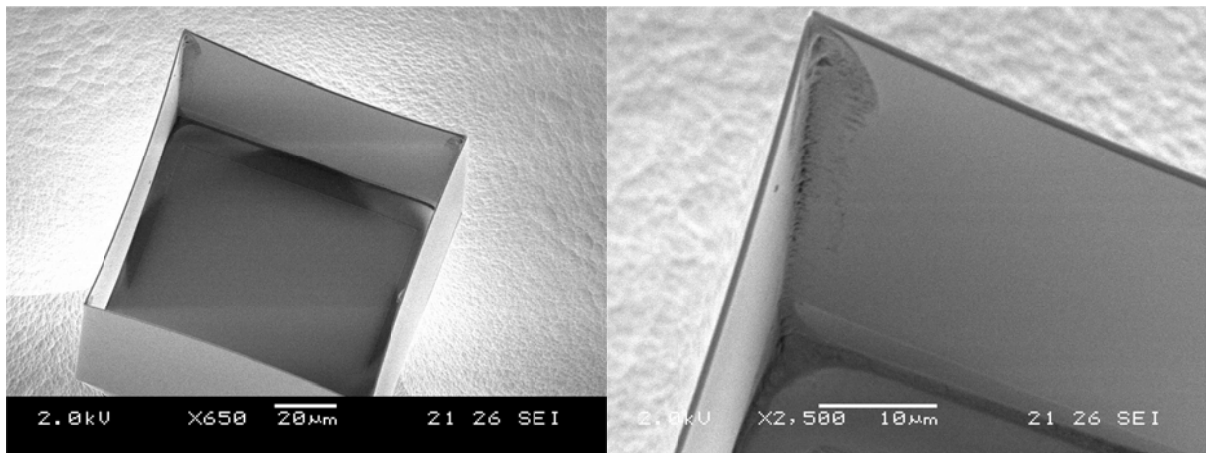


FIGURE 16 GLUING RESIDU IN THE SEAM OF A FOLDED CUBE

Another effect is that the structure fold seamlessly every single time. The flaps move over micrometers and end up seamless over nanometers. This is a huge accuracy that is created by the capillary force. We pushed this effect to the limit by introducing new designs which will test different kinds of distortions. We will change the design in such a way that an additional torsion force is needed to fold seamlessly. This extra hurdle will give us a view on the force that play a role in this folding mechanism.

3 FOLDING TEMPLATES

3.1 METHOD

3.1.1 DESIGN OF THE TEMPLATES

Now we have explained the theoretical model we need to design and construct the templates to verify the model. Design of the templates were done in CleWin and are depicted in Figure 17 and Figure 18. There were different sets of structures with different hinge types. We varied the hinges so that we can experiment with different stiffness's. There are two types of hinges, one type is the solid version, this is a hinge made out of 150nm of SiN. The second type of hinge is also made of 150nm SiN but they are not solid, 8 small hinges connect the flap with a length of 10 μ m. Both these designs are shown in Figure 18. Also the width of these hinges are varied. Every single type of hinge will result in a different β . The varieties of this set is listed in Table 1.

The β of the perforated hinges are proportional to length of the hinges holding the flaps together divided by the total length of structure. So how bigger the holes in the length, how smaller the factor β .

| Type of hinge | Hinge width (μ m) | Flap width (μ m) | β |
|-----------------------------------|------------------------|-----------------------|---------|
| Solid | 3 | 80 | 5,08 |
| Solid | 5 | 80 | 3,05 |
| Solid | 8 | 80 | 1,90 |
| Solid | 15 | 80 | 1,02 |
| Solid | 5 | 50 | 4,88 |
| Solid | 8 | 50 | 3,05 |
| Solid | 12 | 50 | 0,20 |
| 10 μ m hinges | 10 | 80 | 0,24 |
| 10 μ m hinges | 20 | 80 | 0,12 |
| 10 μ m hinges | 6 | 80 | 0,27 |
| 10 μ m hinges , 5 μ m gap | 25 | 80 | 0,07 |

TABLE 1 TYPES OF DIFFERENT HINGES USED FOR DIFFERENT SETS OF STRUCTURES

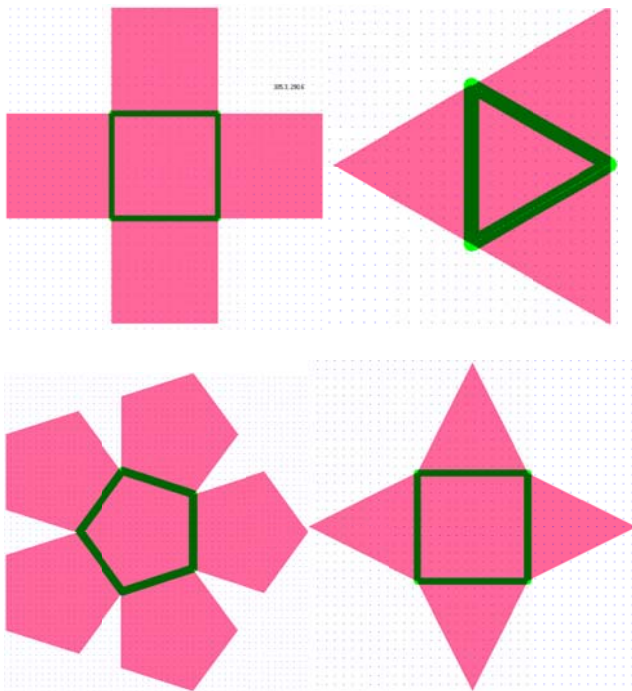


FIGURE 17 DIFFERENT STRUCTURE TEMPLATES, FIRST ONE IS A CUBE, THREE SIDED PYRAMID, HALF A DODECAEDER AND A FOUR SIDED PYRAMID

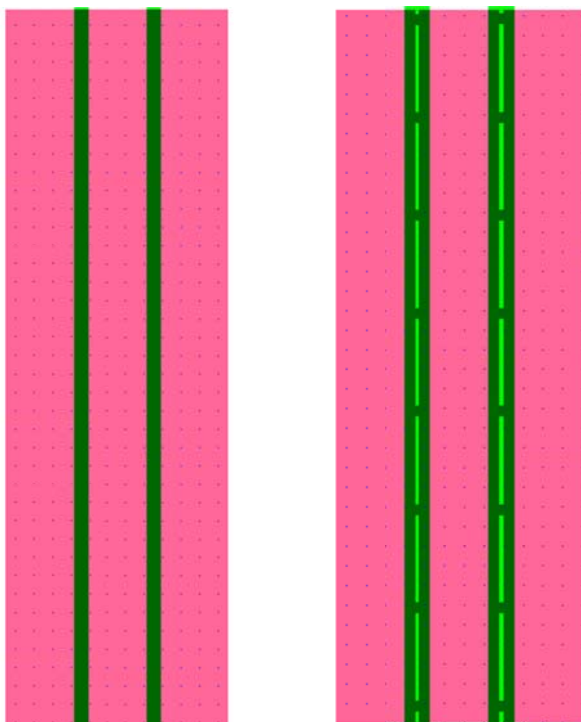


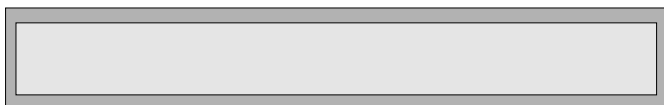
FIGURE 18 DESIGN PRISM STRUCTURE (A) SOLID HINGE (B) HINGE WITH HOLES

3.1.2 CLEANROOM PROCESSES

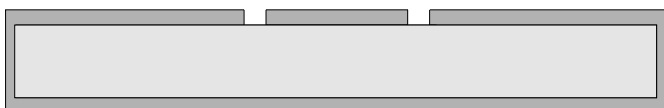
As already discussed the templates are created using contemporary cleanroom processes. The process document for creating these structures can be found in the appendix. Here we can see that the following takes place. On a silicon wafer a SiN layer of $1\mu\text{m}$ is deposited and etched away by plasma etching, leaving grooves for the hinges on the surface of the Silicon wafer. On top of this another SiN layer is deposited of 100 nm. This layer is also deposited between the flaps forming the hinge. Everything but the templates are etched away, leaving a SiN template on the surface of the silicon wafer. The total structure is then isotropically underetched, the left over Silicon form the pillar on which the template rest. Simplified step by step overview is given in Figure 19.



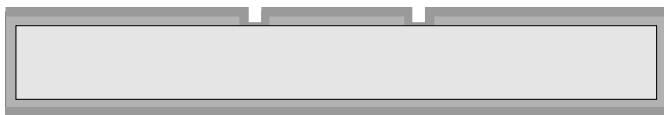
Blank Silicon wafer



Adding SiN layer



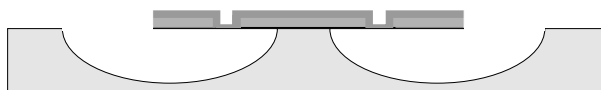
Etching away the hinges



Adding SiN layer



Etching away everything but the template



underetching

FIGURE 19 SIMPLIFIED STEP BY STEP OVERVIEW OF THE PROCESS NEEDED TO CREATE TEMPLATES

3.1.3 EXPERIMENTAL SETUP

To get the structure to fold, one must get a drop of water on the template. As explained before the template is just about $300\mu\text{m}$ in width, and the drop must not be much bigger than that. Therefore the setup has to be created that can dispense small amount of water through a nozzle which is small enough to generate drops of couple of hundreds of micrometers in diameter. To do so we use hollow fibers, one with an outer diameter of $50\mu\text{m}$ and a larger one with an inner diameter of $50\mu\text{m}$, the bigger one is stronger. The thin fiber is slid into the big strong fiber, to form the nozzle. The big fiber is then connected to a pump.

The setup consists further of a table with a microscope. This microscope is placed at an angle of 60 degrees in relation to the table. Previously mentioned fiber is fixed on a probe and fed by a pump with demi water. This probe makes it possible to move the fiber micrometers at a time and maneuver the tip just above the structure. On the microscope a ccd camera is placed, the feed is recorded on the computer.

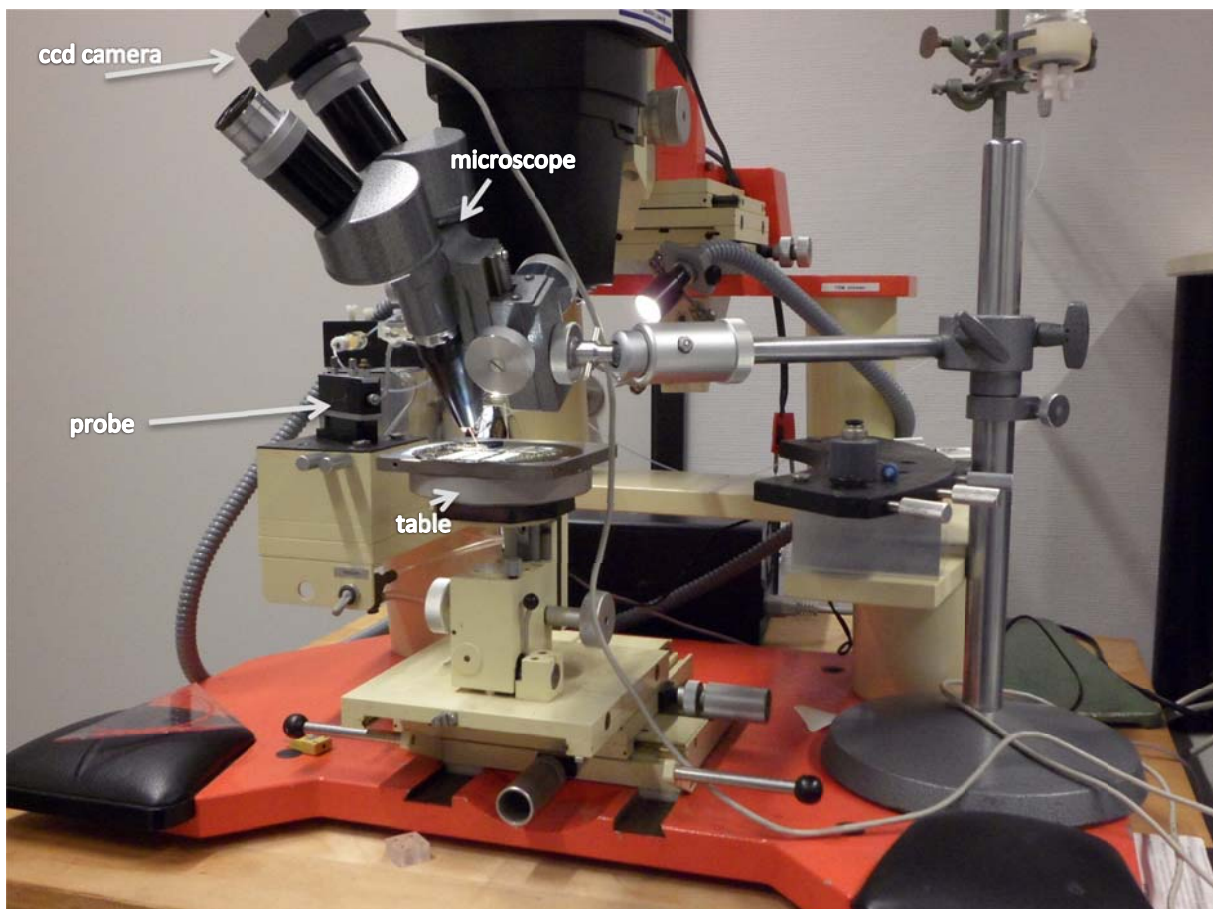


FIGURE 20 PHOTO OF THE SETUP WITH THE IMPORTANT COMPONENTS HIGHLIGHTED

Using this setup we will add a drop of water on the set of structures and create a set of movies of the folding that takes place. We measured the angles that the flaps make with the base of the structure. The angles were measured frame by frame by hand using a computer software. For every flap on every frame we measured three times the angle, the average was taken of these three measurements as the actual angle. These angles were compensated for the viewing angle and plotted in a graph. The question is whether we can reconstruct the model as discussed in the previous chapter using these experimental results.

3.2 RESULTS

3.2.1 FIRST RESULTS FOLDING STRUCTURES WITH MORE THE 2 FLAPS.

First experiments on these were not that successful. Although the group had successfully folded a cube it was not reproducible in the amount of time I took to do the experiment. There were some phenomena that are remarkable.

Some structures had stiff hinges due to design and didn't fold into the full structures but they bended a little. Confirming that the folding angle would increase when the hinges are less stiff. Folding action also works the other way around. When administering an amount of water into the cavity below the structure the flaps of the structure floated on the surface of this puddle. When this puddle dried up the flaps followed the surface of the puddle downward. So we had downward folding. After all the water had evaporated the flaps jumped back into their original position. This last observation contradicts the observation of the cube that was folded. This cube held its form even when the water was evaporated. See Figure 5d.

If water is added to the cavity the flaps will float on the surface of the water and when the water evaporates the flaps will fold down as shown in Figure 21. After all the water is evaporated in the cavity the flaps will bounce back to their original state.

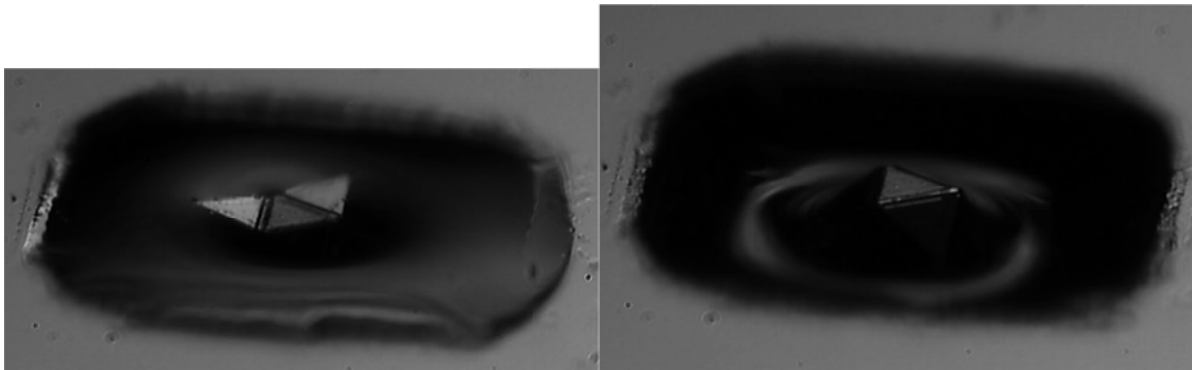


FIGURE 21 TRIANGLE PYRAMID WITH WATER IN CAVITY, (B) THE WATER IN THE CAVITY IS PULLING THE FLAPS OF THE TEMPLATE DOWN

3.2.2 RESULTS OF FOLDING OF PRISM

Initial folding of prisms was a success. It is fairly easy to place a drop on the structure with the setup. While the heat of the lights made the drop evaporate it was clear that the flaps bended and at some type of hinges even folded completely. The set with the array of $10\mu\text{m}$ hinges folded all completely. Frame by frame analysis of the movies taken showed that the angle of the flaps increased until they closed seamlessly. Measurements are shown in Figure 22. The measurement is done at both flaps, and the angle of the flaps in relation to the center flap is measured. The measurements are compensated for the angle of the microscope. On every frame three measurements were taken per flap and averaged. Table 2 is similar to Table 1 but we added whether the structure folded fully.

We did see some phenomena worth mentioning, the structures that folded completely, folded seamlessly as well. This happened every time. The meniscus of water guided both edges of the flaps to each other. So the edges were pulled together by the capillary forces, and the structure folds seamlessly.

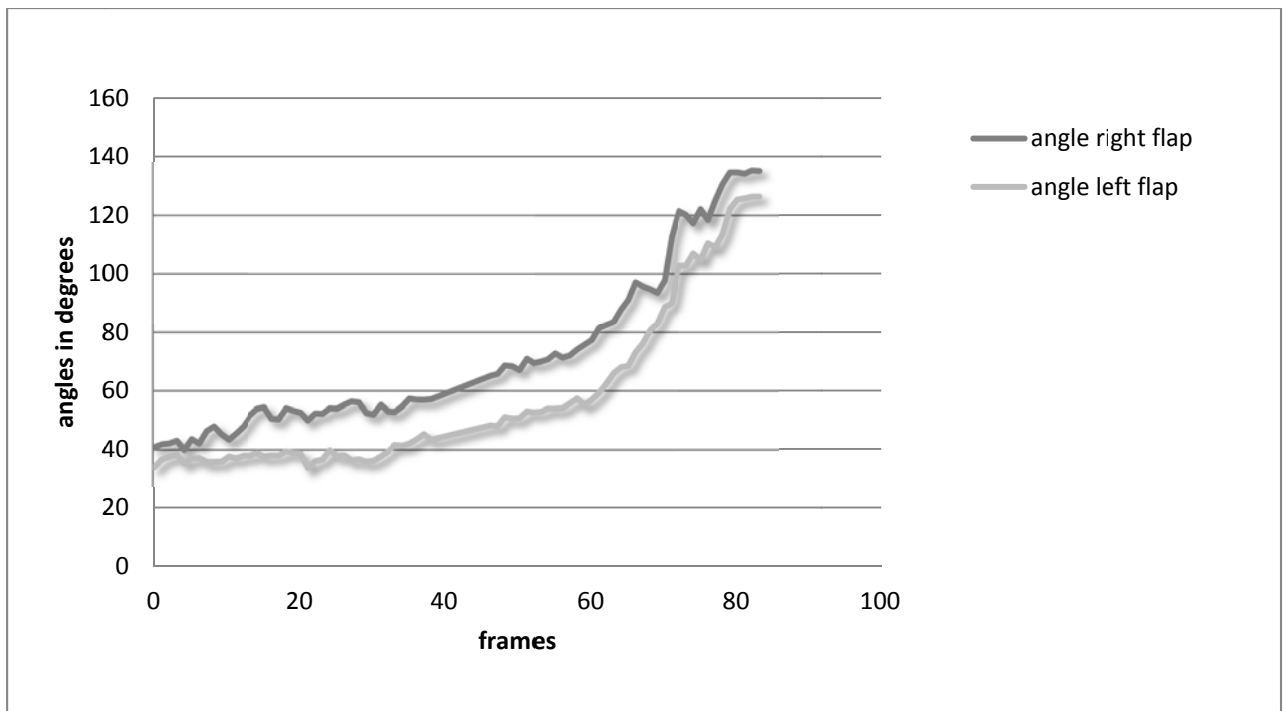


FIGURE 22 MEASUREMENT OF FULLY FOLDING, TAKEN FROM A MOVIE THAT PROGRESSED 5 FRAMES PER SECOND.

Other hinges which were solid and were narrow were too stiff for fully folding. Figure 23 shows the measurement done on a structure that doesn't fold completely. The table beneath this figure shows which structure behave in which manner. In this case a maximum angle of 32 degrees is achieved by both flaps.

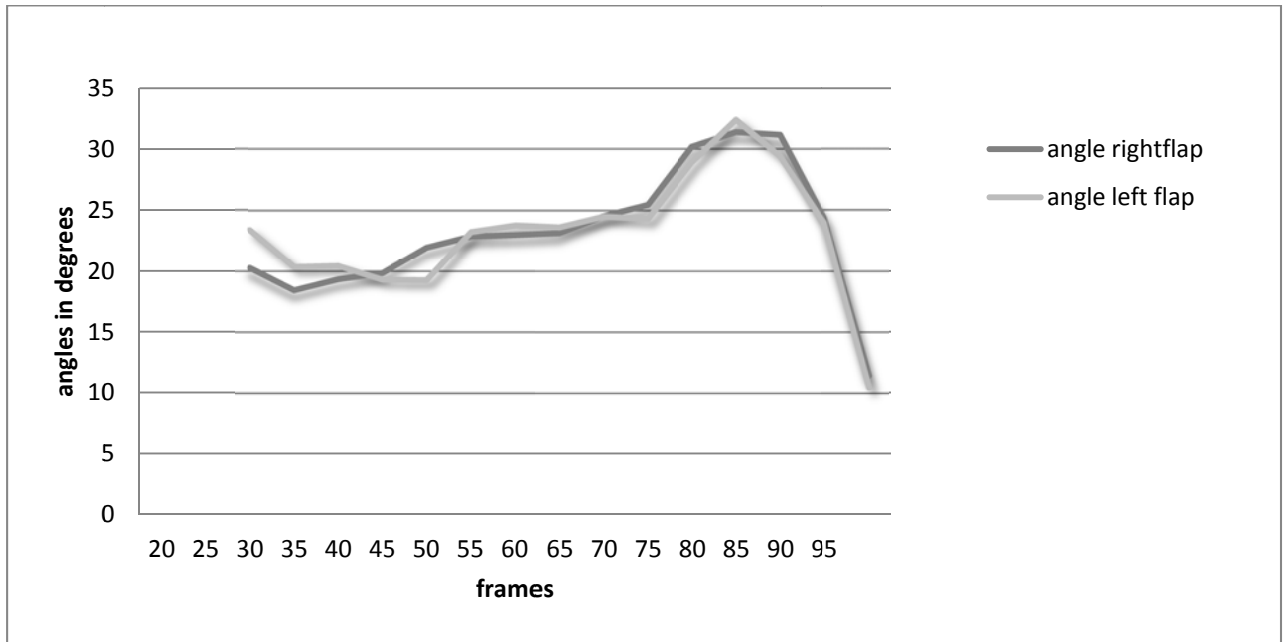


FIGURE 23 MEASUREMENT OF FOLDING AND OPENING, TAKEN FROM A MOVIE THAT PROGRESSED 5 FRAMES PER SECOND

| Type of hinge | Hinge width | Flap width (μm) | β | folding |
|---|-------------|------------------------------|---------|---------|
| Solid | 3 | 80 | 5,08 | |
| Solid | 5 | 80 | 3,05 | |
| Solid | 8 | 80 | 1,90 | |
| Solid | 15 | 80 | 1,02 | Fully |
| Solid | 5 | 50 | 4,88 | |
| Solid | 8 | 50 | 3,05 | |
| Solid | 12 | 50 | 0,20 | Fully |
| 10 μm hinges | 10 | 80 | 0,24 | Fully |
| 10 μm hinges | 20 | 80 | 0,12 | Fully |
| 10 μm hinges | 6 | 80 | 0,27 | Fully |
| 10 μm hinges , 5 μm gap | 25 | 80 | 0,07 | Fully |

TABLE 2 FOLDING OF DIFFERENT STRUCTURES

We can convert the measurements done frame by frame, a time progression, in to a measurement done on variation of the water volume. This is exactly how we setup the theoretical model and these measurements will give the measurement point for constructing the graph shown in Figure 24.

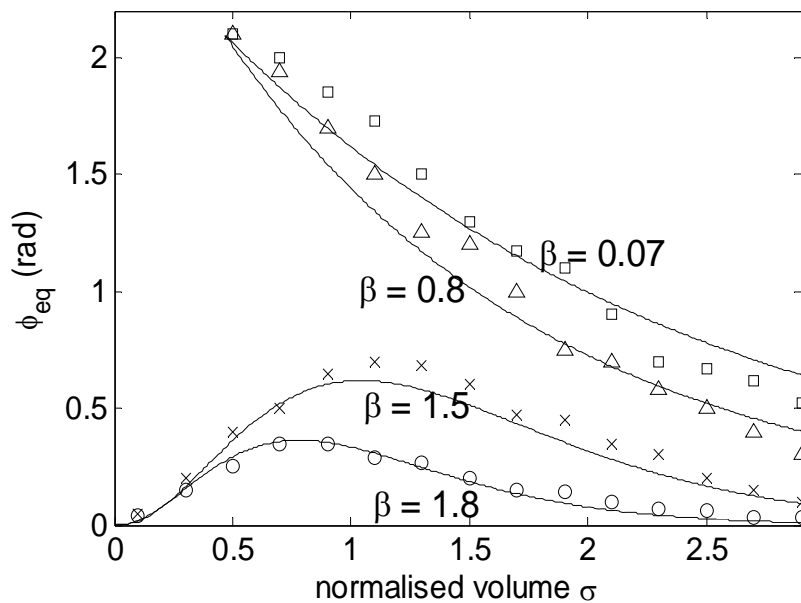


FIGURE 24 MEASURED PHASE DIAGRAM OF THE EVOLUTION OF EQUILIBRIUM STATES AS FUNCTION OF VOLUME (4)

It is striking that the simplification of the model has so little influence that the actually measured values correspond almost exactly to the model. Simplifications like totally ignoring a whole dimension do not make the theoretical model deviate from the measured values.

4 FOLDING WITH DIFFERENT CONTACT ANGLE

4.1 METHOD

To determine the effects of a defined contact on the folding of the structure we need to use liquids that have a defined contact angle on SiN. Or we need to change the surface of the SiN so that water has a contact angle on the this surface. After drafting a list of liquids with different contact angles we came to a conclusion that not all liquids were appropriate to use in my setup due to safety reasons.

Changing the property of a surface can be done by depositing a layer of Fluor Carbon. Fluor Carbon is hydrophobic and the thickness of the layer determines the amount of hydrophobeness and thus the contact angle of the liquid on this surface. A layer of FC can be deposited by using a Reactive Ion Etching chamber (RIE) (5).

The results of some reference experiments done on an empty silicon en SiN surface are depicted in Figure 25. We decided to do the folding measurements by putting the samples in the RIE chamber between 0 and 10 minutes.

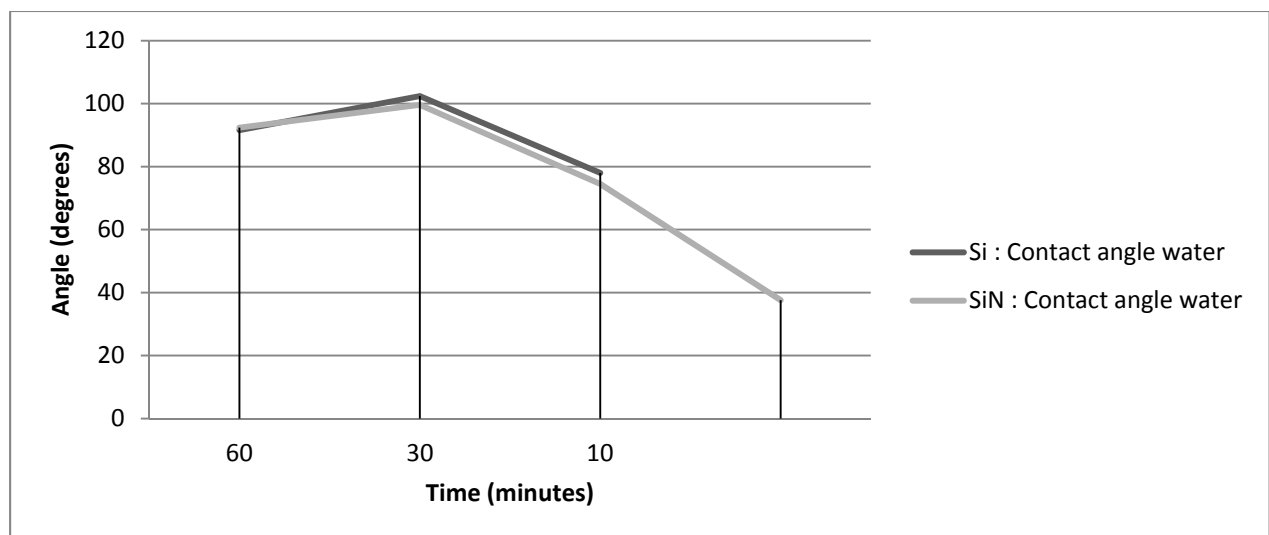


FIGURE 25 VARYING OF CONTACT ANGLE DUE TO TIME OF FC DEPOSITION

Changing the surface into hydrophobic means that the drop of water coming from the fiber might cling to the fiber and not want to stick to the surface. To overcome this we have coated the fiber also with FC, this is done by submersing the fiber into liquid FC. The fiber did not clog by this layer of FC.

4.1.1 WHITE LIGHT MEASUREMENT USING LATERAL SCANNING INTERFEROMETRY

To change the contact angle we chose to deposit a FC layer onto the structures. The question rised whether the flaps on the structure would bend to the extra force asserted by the elasticity of the FC layer. To measure whether this is the case, whitelight measurements using lateral scanning interferometry were conducted on the structures. This will give a clear indication of the orientation of the flaps. The interferometer measures the horizontal distance of the surface.

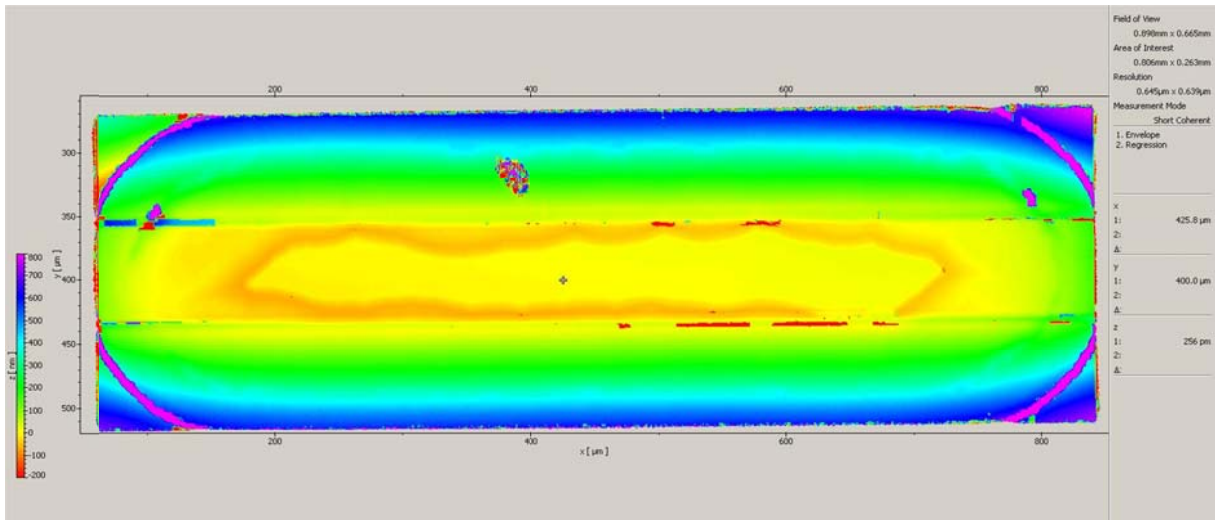


FIGURE 26 INTERFEROMETER MEASUREMENT OF THE FLAPS

Figure 26 shows one of the actual measurement done on the structures. There was an average increase of the angle of the flaps of 0.06 degrees. This we concluded as neglectable. This means that adding a layer of FC will not additionally increase the angle of the flaps.

4.2 RESULTS

We did the same folding experiments as in the previous experiments, and this time we looked only to the maximum ϕ_{eq} of each set. We got similar results as shown in Figure 22 and Figure 23, and from these results we looked at the maximum angle attained. We managed to do this experiment for two different hinge stiffness's. The results of the measurement are depicted In Figure 27. The solid line is the theoretical and expected progression of ϕ_{eq} to variation of the contact angle ϕ_c . The crosses are the measured points.

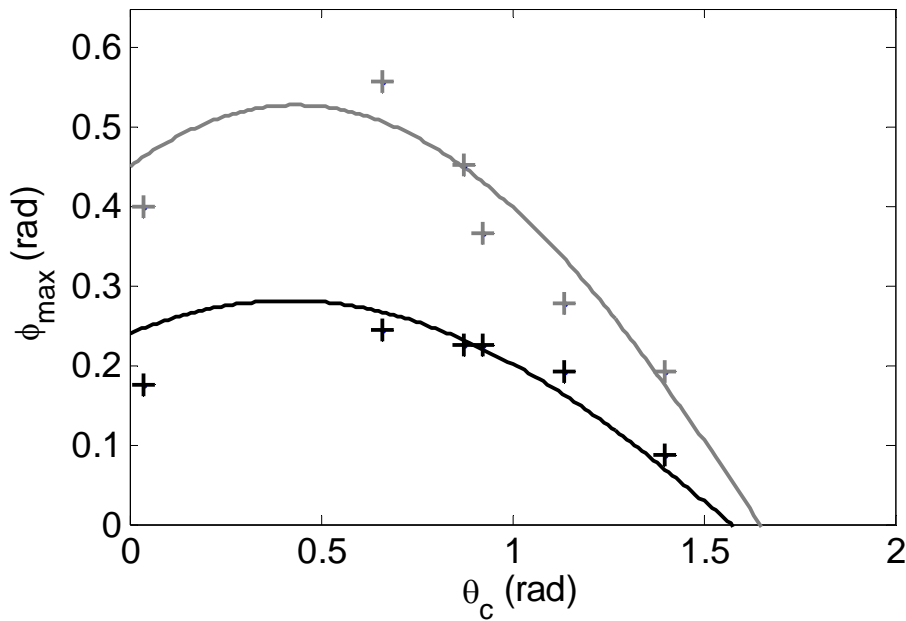


FIGURE 27 MAXIMUM ANGLE FOR DIFFERENT CONTACT ANGLES (4)

Again it is striking that we get measurements that fit the model despite of the simplifications. We actually conclude that capillary properties do follow the model, and thus this process is predictable and useful for fabrication of three dimensional structures on this scale.

5 VARYING DESIGN OF THE PRISMS

5.1 PROBLEM DEFINITION

5.1.1 TORSION IN FOLDING

We have seen that every time the prism fold the fold seamlessly. To put this to the test we have made some hurdles. One of these hurdles is to see whether the capillary forces will overcome the rotational forces in the lateral direction. In other words if we design flaps of the prism with decreasing flap width over the length as shown in Figure 28 will the structure fold seamlessly. This would result in a folding like shown in Figure 29 if the structure would close seamlessly, at the front where the width is D2 the hinges would stretch out and at the rear where the structure was D1 in width, the hinge would be pressed downwards. adding extra strain on the folding process Other scenario for this design is that the hinge would not give way and the structure won't close seamlessly, and may open again.

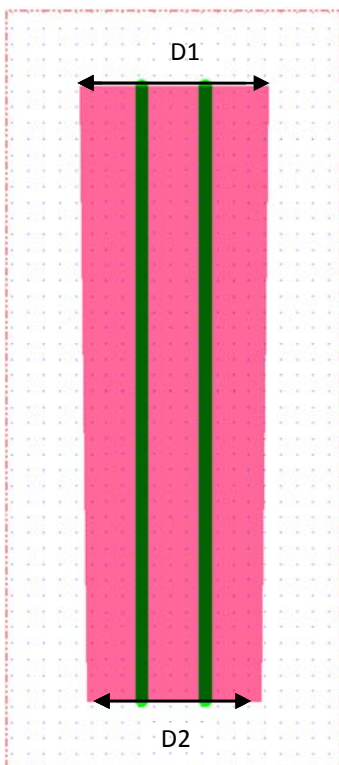


FIGURE 28 STRUCTURE WITH DECREASING FLAP WIDTHS

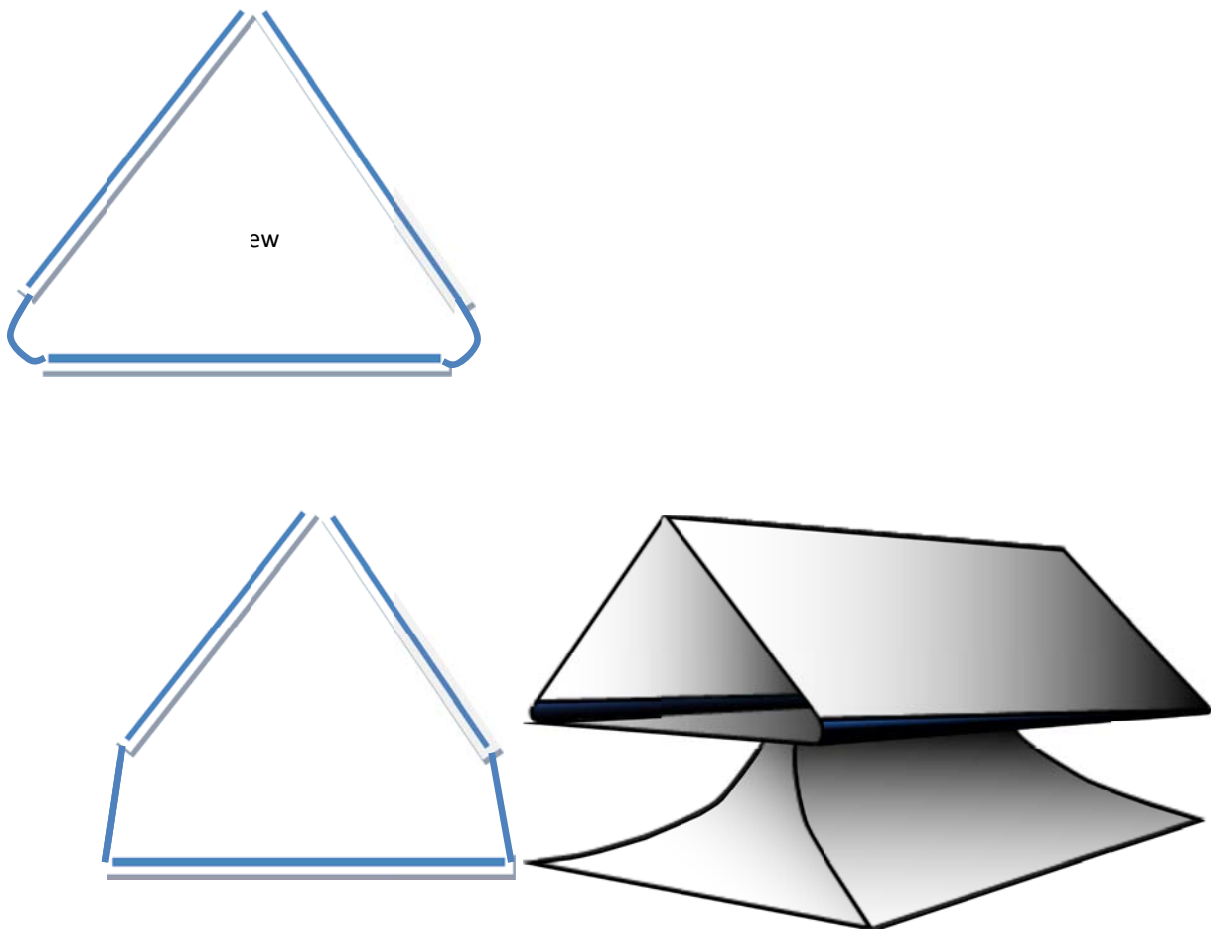


FIGURE 29 DISTORTION OF THE HINGES

The difference between $D1$ and $D2$ are not more than the hinge width of $5\mu\text{m}$. This is chosen so that there will not be any influence of other effects other than the bending and stretching of hinges.

5.1.2 FOLDING WITHOUT SYMMETRY

Next set of structures have flaps of different width, the left flap will have a smaller width than the right one as shown in Figure 30, the width $D2$ is larger than $D1$. Again we will test whether these flaps will fold seamlessly. And if they do they can fold in two ways, the ends of the flaps meet each other, or one end of the flap will meet halfway of the other flap as shown in Figure 31. In the first case both the angles of the flaps will be the same, in the second case the angles will be different, ϕ_1 is not equal to ϕ_2 .

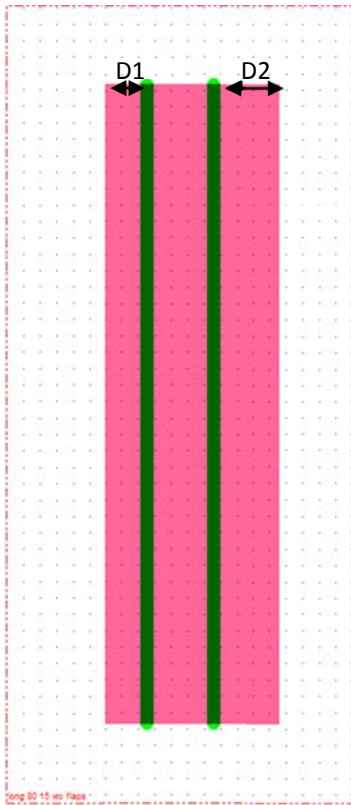


FIGURE 30 STRUCTURE WITH DIFFERENT FLAP WIDTHS

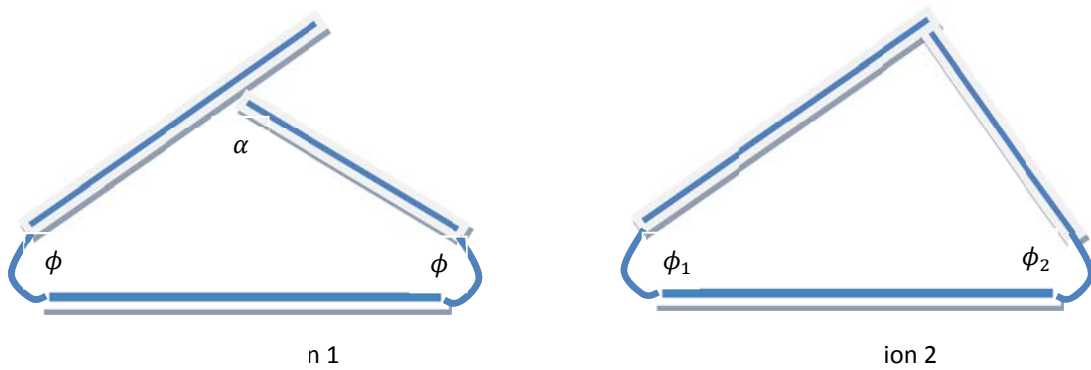
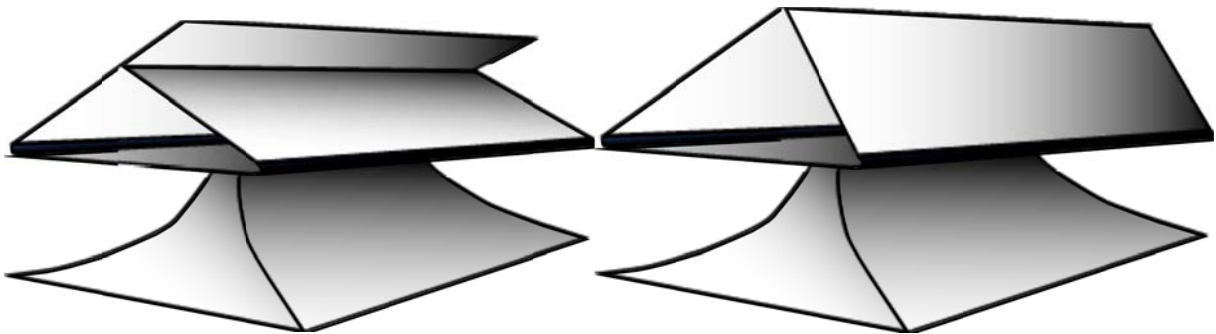


FIGURE 32 (A) STANDARD 45 ANGLE EDGE (B) FLEXIBLE EDGE

5.1.3 VARYING CONTACT AREA

Third type of structures will have a varying contact surface. Previous experiments have shown that folded structures tend to stay folded despite of the elastic forces in the hinges. To test this phenomena we will vary the contact surface of the flaps and we will vary the elasticity of the hinges . We will try to determine which hinge stiffness and contact area combination will be on the transition of structures always staying folded to structures folding and opening again. This will give us information of the quantity of the forces keeping the structures together.

We will create three sets of three different contact angles. Every set consists of twenty variations of d where d is varied from $20\ \mu\text{m}$ to the full $390\ \mu\text{m}$.

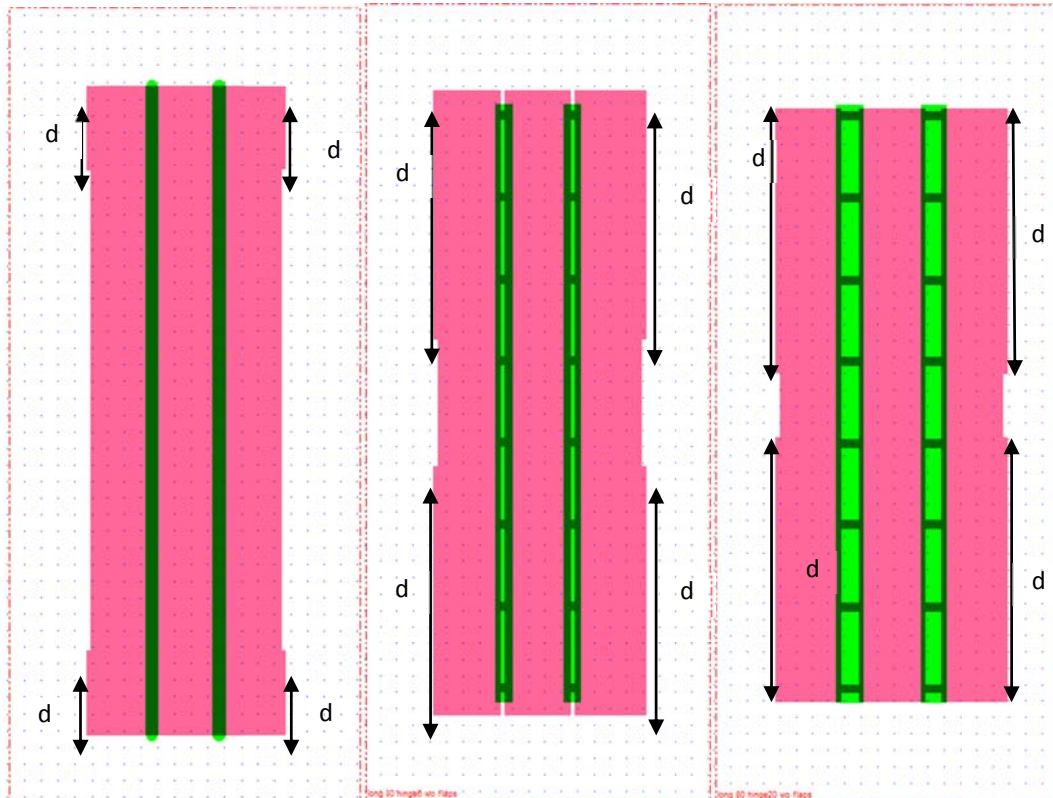


FIGURE 33 STRUCTURE WITH VARYING CONTACT SURFACE

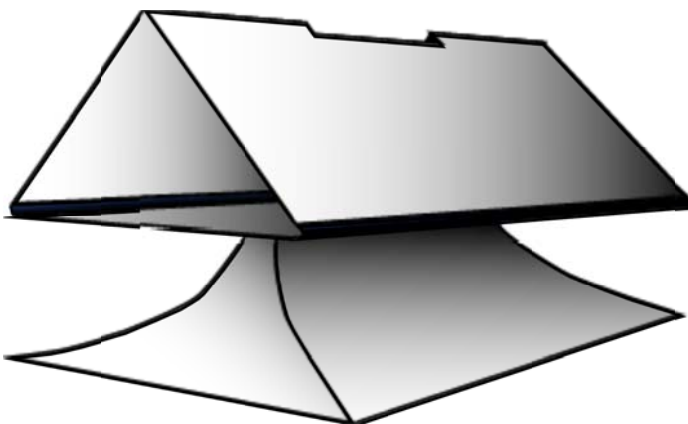


FIGURE 34 STRUCTURE WITH VARYING CONTACT SURFACE FOLDED

5.1.4 LIFTING OBJECTS OUT OF THE PLANE

Last but not least we will try to lift a structure of the surface using this folding action. For this experiment we created structures with the letters of the university on the flaps. When the flaps fold these letters will be lifted from the plane and we will have a micro billboard. In the same time that the flaps are under etched the letters will be etched free from the underlying silicon, and thus hang freely like the flaps.

This design has a small hole in the extension that is holding the letter. This hole is made for the under etching to perform well. Without the hole the addition to the structure which holds the letter can cause the under etching not to free the right flap from the center flap as shown in Figure 36. The hole will make it possible for the etchant to reach in the center of the arm. In this figure the white shape is the structure that is left after underetching. This structure supports the flaps that lay on top.

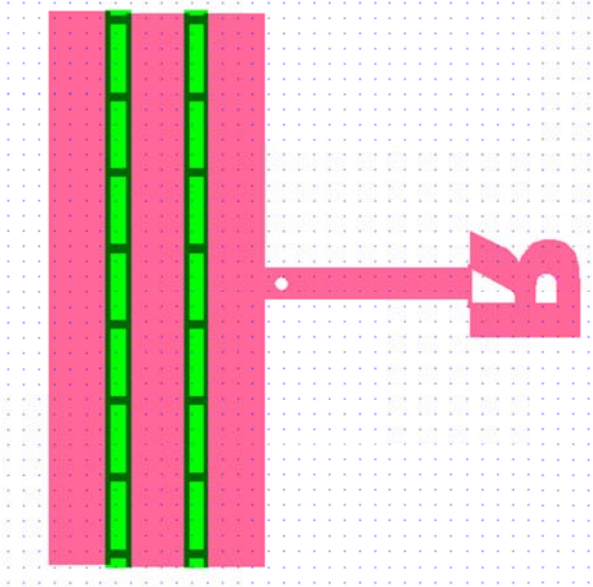


FIGURE 35 STRUCTURE WITH A LETTER

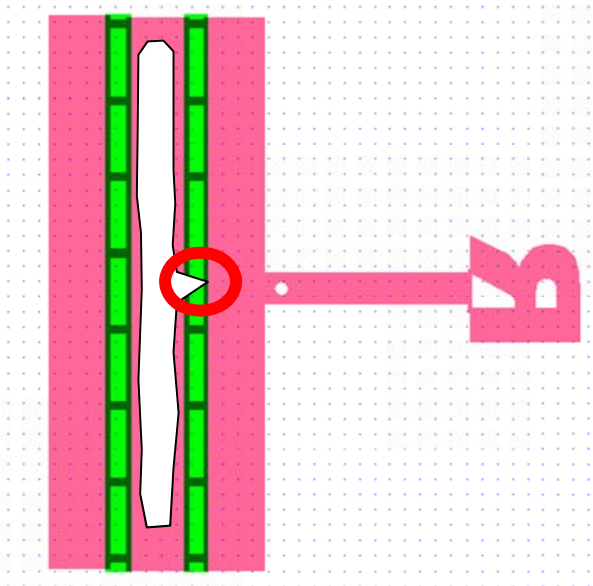


FIGURE 36 WHERE IT CAN GO WRONG WITH UNDERETCHING

5.2 RESULTS

5.2.1 TORSION IN FOLDING

Folding experiments confirm seamless folding. This means that the hinges stretch and fold where needed to facilitate this. We can conclude that the capillary forces are large enough to force the hinges.

5.2.2 FOLDING WITHOUT SYMMETRY

Folding with flaps of different widths resulted in some remarkable results. As already stated in the previous chapter the folding could have gone in two ways. From the measurements of the optical microscope it looked like that the folding occurs in the manner as depicted as option 2 in Figure 32b. Further experiments revealed the full extent of the mechanics in this folding.

In the very first measurements we saw that the flaps will take a maximum angle and fold back when the hinges were stiff enough. This is due the torque on the flaps. We have determined that the capillary effect administers a force on the flaps, the folding occurs not when the this force is larger than the counter acting elastic force of the hinges, but when the width of the flaps times the capillary force is larger than the elastic force. This means a fully folding structure won't fully fold when the flaps are made less wide. This is shown in Figure 37.

Another way to explain this is by using the model we used in the previous chapter. We have a factor β which is dependant on the width of the flaps w : $\beta = \frac{B}{\gamma w l_0}$. This means that when we change the w we change the folding property of the flap. In this case in such a way that it will not bend through to close.

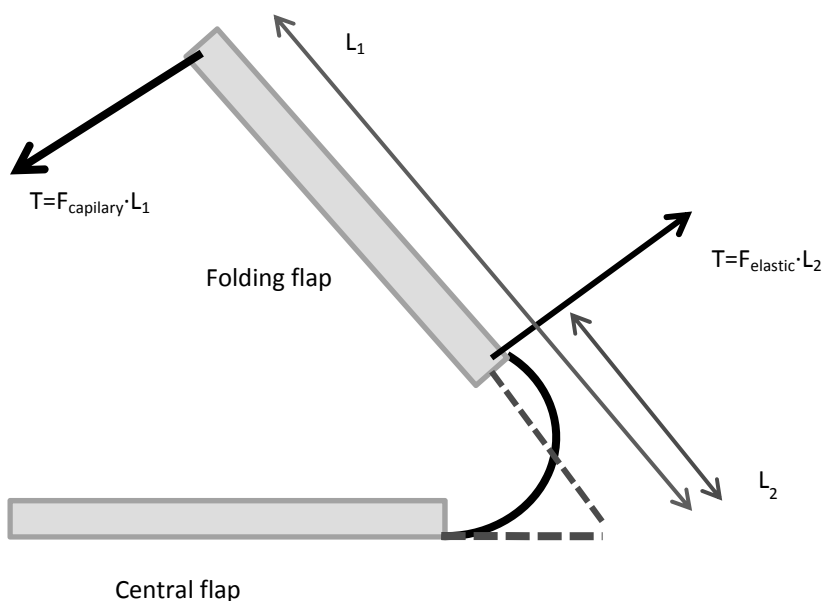


FIGURE 37 CAPILLARY FORCE VS ELASTICITY FORCE, THIS SIMPLIFIED MODEL SHOWS HOW TORQUE IS RELATED TO THE LENGTH OF THE FLAP.

We have witnessed that a smaller flap takes a maximum angle, while the normal and larger flap keeps folding and then crashing into the flap with the maximum angle. The larger flap doesn't have the width to fold seamlessly over the a flap that would stop the folding. This shown in frames taken from a measurement in Figure 38. Here you can see that the right flap stays on the same angle while the left flap keeps on folding, in the end it will collapse and not stay folded.

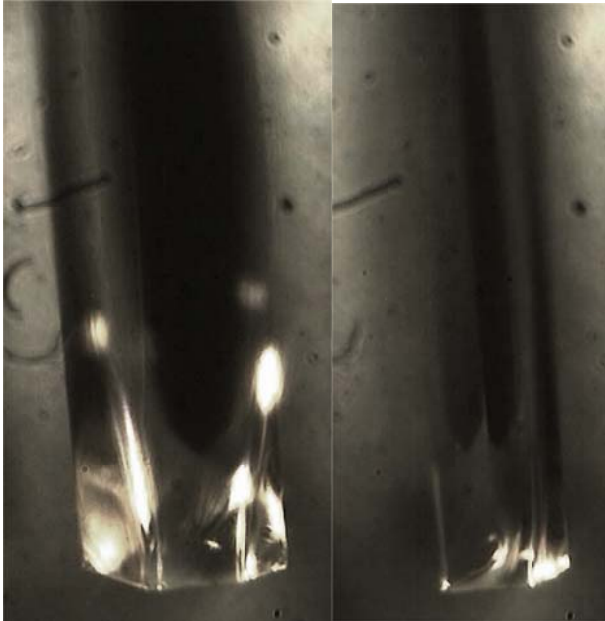


FIGURE 38 ASYMETRIC FOLDING, RIGHT FLAP REACHES A MAXIMUM ANGLE AND STOPS FOLDING

Although the width difference between flaps in this figure is dramatic, this phenomena occurs also in structures which appear to fold normally (Figure 39), where the difference in width are not that dramatic as shown in the previous example, under a SEM the it is clear that the left flap crashed into the right flap that stood steady on a maximum angle, this is shown in Figure 40.

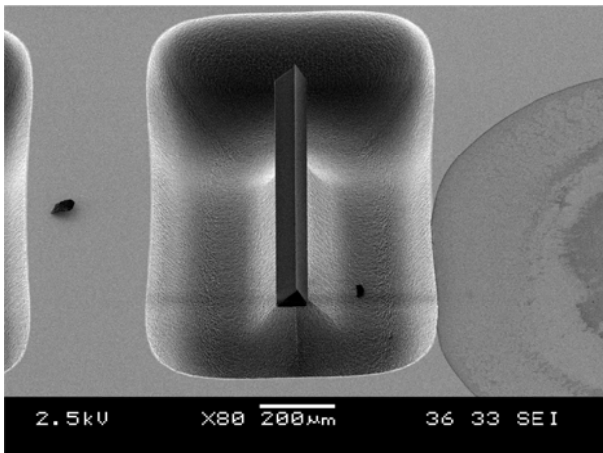


FIGURE 39 SEM PICTURE OF ASYMETRIC FOLDED STRUCTURE

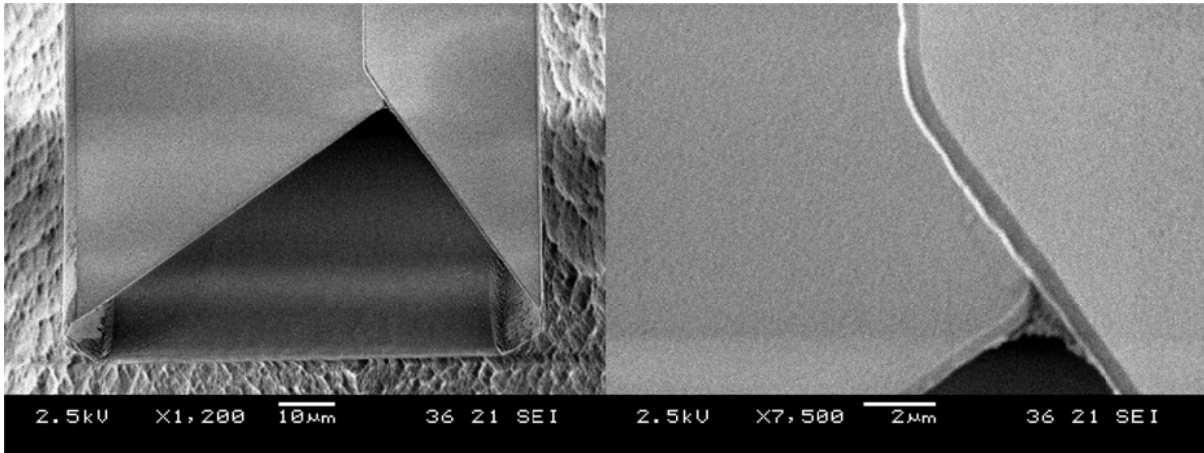


FIGURE 40 CRASHING PHENOMENA, RIGHT FLAP REACHED A MAXIMUM ANGLE AND THE LEFT FLAP CLOSED INTO THE STEADY RIGHT FLAP.

5.2.3 VARYING CONTACT AREA

This experiment consisted of three sets, with three different hinge types. Every set had twenty variations of the contact area and every variation was repeated ten times in ten rows. The hinges with holes in them folded and stayed folded for all contact areas. So we can conclude that the hinges weren't stiff enough. The set with the solid hinge resulted in all structures opening for all contact area's except for contact area's larger than $720 \mu\text{m}^2$. Only three types of structures fell in this category. Repeating this experiment for the ten identical structures revealed that due to the manufacturing process there is a deviation. The first three rows open at $720 \mu\text{m}^2$ the last 7 structures open at $680 \mu\text{m}^2$. Because the majority of the structure only stay closed with a contact area of $720 \mu\text{m}^2$ and we assume that the deviation is due to production process we will take this value to be used in the calculations.

This mean that for the energy

$$U_b = \frac{1}{2} \frac{B}{l_0} \theta^2$$

Where $B = \frac{EA^3}{12(1-\nu^2)} \approx 10^{-10}$ and with $\theta = 2/3 \pi \approx 2$ we get $U_b = 4 \cdot 10^{-5} \text{ J/m}^2$. For a contact area of $720 \mu\text{m} \times 1 \mu\text{m}$ this is an equilibrium point, this means that a structure that folds seamlessly over the whole length of $800 \mu\text{m}$ leads to $4.4 \cdot 10^{-5} \text{ J/m}^2$. This is the minimum energy per square area needed to keep the structure folded, and gives us a measure for the forces that the gluing substance has to assert.

SEM pictures of folded structure with reduced contact area is shown in Figure 41. For any larger hole in the middle the flaps will not stay closed.

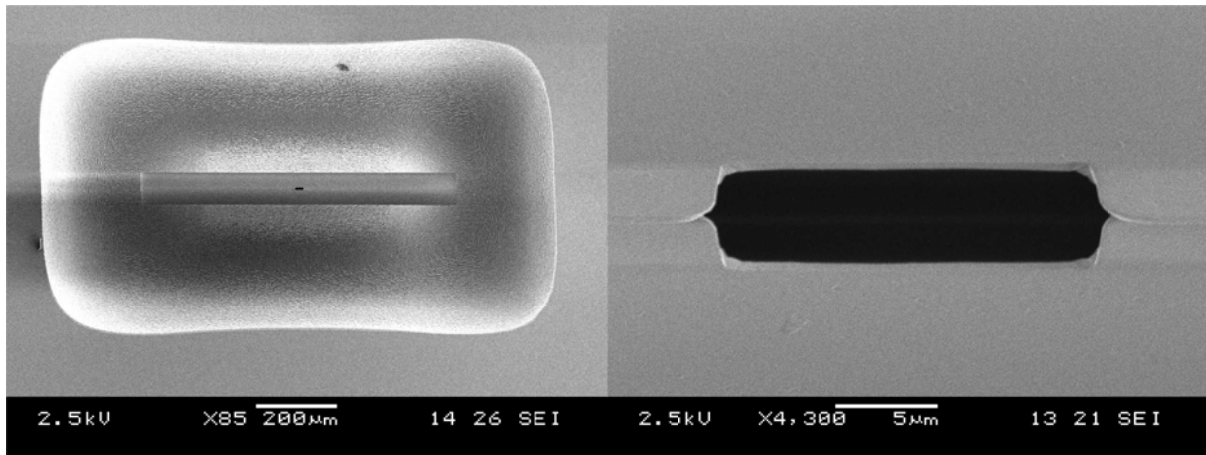


FIGURE 41 FOLDED STRUCTURE WITH SMALLER CONTACT AREA

There was an unexpected effect while doing these experiments. As shown in Figure 42 there is bending in the middle of the folded flaps for very large gaps. A SiN flap of 80 by 725 µm is very rigid. To deform this flap we need a large force.

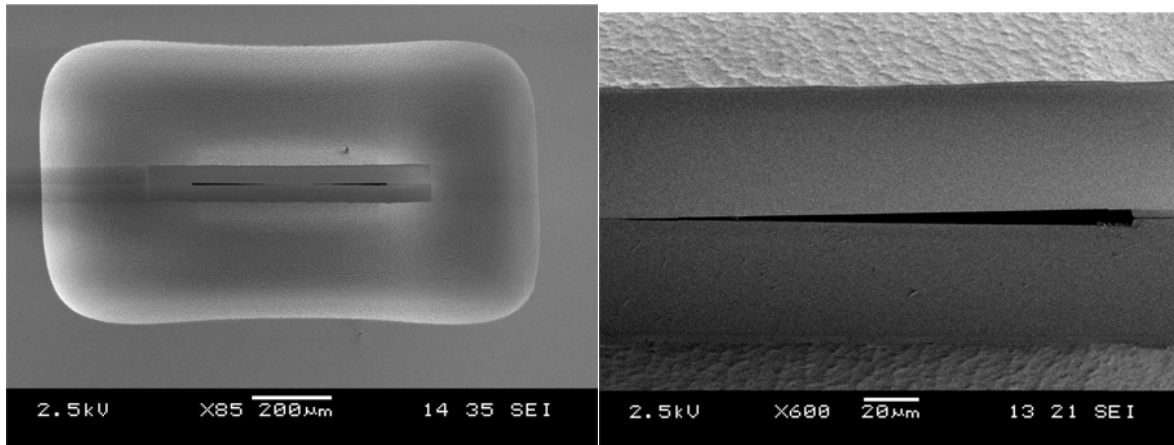


FIGURE 42 BENDING IN THE MIDDLE OF FOLDED STRUCTURES

We made an estimation by taking using the Euler-Bernoulli equation:

$$\frac{\partial^2}{\partial x^2} \left(EI \frac{\partial^2 w}{\partial x^2} \right) = q$$

Where $w(x)$ describes the deformation along the x direction of the flap, q is the distributed load (force per unit length). E is the Young's modulus and I is the second moment of area. In this case $I = \frac{1}{12} h^3 b$, where h is the height when taking the crosssection of a flap, 1 µm and b is the width of the flap: 80µm.

The distortion is approximated by a 4th order polynomial: $w(x) = -Ax^4 + Bx^2$. Solving this function when requiring $w'(0) = 0$, $w'(-\frac{1}{2}L) = 0$, $w'(\frac{1}{2}L) = 0$, $w(0) = 0$, $w(-\frac{1}{2}L) = u$, $w(\frac{1}{2}L) = u$, we acquire expression for $w(x) = -\frac{16ux^4}{L^4} + \frac{8ux^2}{L^2}$. Here u is the distortion, L is the length of the flaps and x the position on the length of the flaps. Figure 43 shows the $w(x)$ when the values are filled in. Now that $w(x)$ is known we find $q = \frac{-384EIu}{L^4}$. We measure a maximum distortion of 2.4µm from Figure 42. Filling in the values for the dimensions we get 602 N/m for q . This model assumes that the whole flap bends as a whole, and the bending is the same of the whole width. If you look carefully you might see that in Figure 42 the bending on the edge is

larger than the bending on the hinge side. This is to be expected because on this side the hinges pull on the flaps. We redo the calculation for the amount bending as it is on the hinge side of the flaps, which is $1.67\mu\text{m}$, resulting in a q of 419N/m . We take the average value as good estimation of the force asserted on the flaps: $510,5\text{ N/m}$ Multiplying this with the length of the structure of $720\ \mu\text{m}$ results in a force of 0.37 N . Which is really large for such small device.

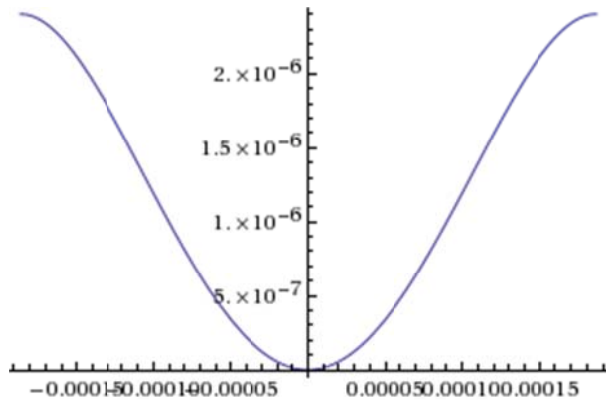


FIGURE 43 APPROXIMATION OF THE DISTORTION

1572 N/m^2 . This is a much smaller than the adhesion force, and we must conclude that other forces play a role.

We need to keep into account the torque that is asserted on the structure. Figure 37 shows how momentum is related to the distance over the flap. So when we compare two different forces on this structure we need to look at the torque on the right location of the structure. If we take the factor $\frac{L_2}{L_1}$ times the force at the edge of the flap, 510.5 N/m we get a force of 36.5 N/m at L_2 . To calculate the torque we need to calculate the energy using the formula for energy U_b , where $\vec{F} = \vec{\nabla} \cdot U_b$. So this gets us a F of 7.5 N/m . When taking this for the whole length of $800\mu\text{m}$ and then dividing by the minimal surface that need to keep the flaps together ($720 \times 1\ \mu\text{m}^2$) we get $0.83 \cdot 10^7\text{ N/m}^2$ for the adhesive force needed to keep the flaps together.

If we compare this force with van der Waals force, which is given as $F = \frac{A}{6\pi h^3}$ (6), where A is the Hamaker constant which is between 10^{-19} and 10^{20} , and h is the surface separation between two plates. The surface separation is the roughness between two plates and in our case we will assume it 15nm . This results in a force of 1572 N/m^2 . This is a much smaller than the adhesion force, and we must conclude that other forces play a role.

5.2.4 LIFTING OBJECTS OUT OF THE PLANE

As you might have seen on the cover and in Figure 44b, this experiment was a success as well. After lifting the letter with the same experimental setup as used in the whole project we made Scanning Electron Microscope images of the lifted letters.

Figure 44b shows the hole we made in the design so that underetching would free the arm. The effect of this underetching through this hole can also be seen in this figure as I have highlighted it with a white circle.

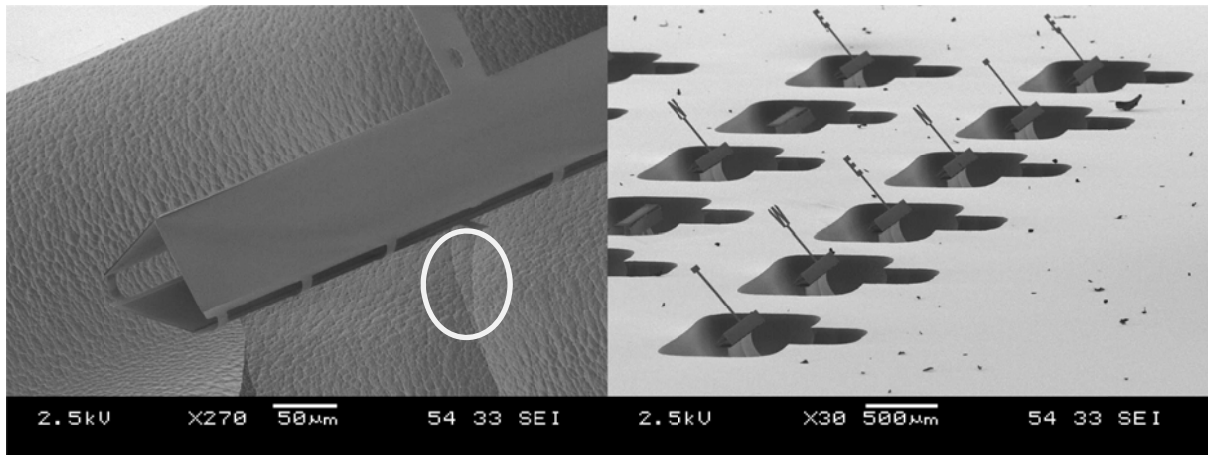


FIGURE 44 (A) HOLE IN THE ARM WAS NEEDED FOR ETCHING FREE THE ARM WITH THE LETTER (B) LIFTED 'LETTER 'TWENTE'

If lifting fails the structure won't return to its original position because water will come under the structure and pull the letter to the floor of the cavity, and gluing the letter to the floor. Results of this is shown in Figure 45a.

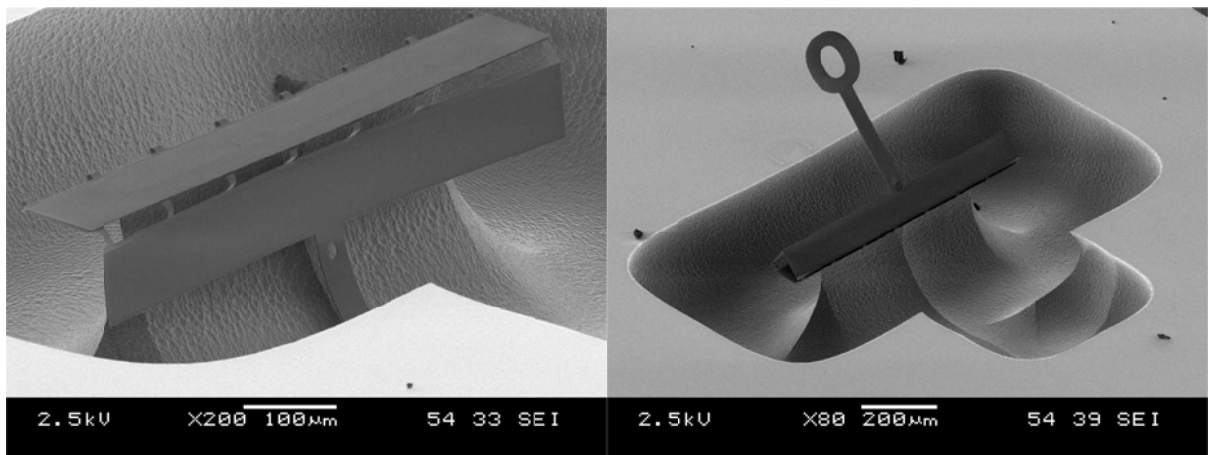


FIGURE 45 (A) LIFTING OF LETTER FAILED (B) LIFTED LETTER O

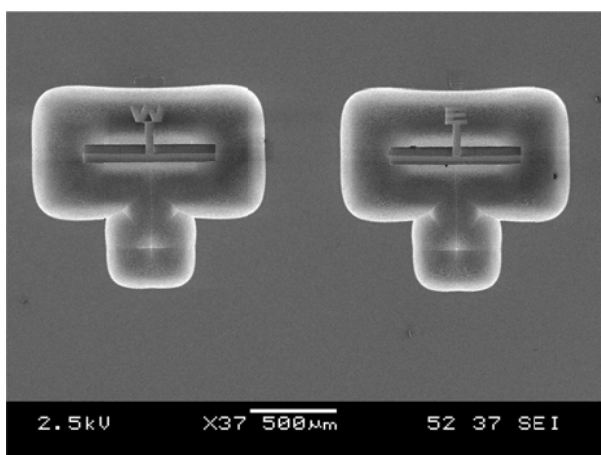


FIGURE 46 TOP VIEW OF LIFTER LETTERS

6 CONCLUSION

In earlier work it was already proven that folding with capillary forces is a easy and predictive way to create three dimensional micro structures. But these works were with liquids that solidified and were left behind in the structure. The decision was made to overcome this by using demi water for folding. Which would evaporate totally and leave nothing behind. A theoretical model was made for predicting the folding behavior of the structures.

From experiments it was clear that the folding mechanism followed the theoretical model almost to the letter. Experiments done with variation of the contact angle by changing the surface characteristics of the structures revealed the folding progression followed the deviations as expected in the theoretical model. Experiments with varying contact angles revealed that the capillary force is 70 times larger than the force asserted by the hinges. Making them ideal for folding.

The choice for using water was made because in theory nothing will be left behind in the structures because the water evaporates. In our experiments it became clear that a residue is left in the seam of the structures. Further experiments revealed that this residue has an adhesive force of $0.83 \cdot 10^7 \text{ N/m}^2$. Which is much larger than the van der Waals power, which is 1571 N/m^2 . So we can conclude that other forces play a role in this adhesion.

We need to determine what this consists of. One might think of a combination of adhesive forces of the material with for example electrostatic forces. Further experimentation is needed.

Experiment with contact area variation resulted also in an unexpected bending of the flaps. As shown in Figure 42. We estimated the force needed to bend a flap as 0.37 N. Illustrating once again that the capillary forces are really large.

When the structures fold completely, every single time the flaps of the structure folds seamlessly. To test this further new structures where created with varying flap widths over the length. Still the flaps folded seamlessly, meaning that the hinges were stretched out on one end and folded on the other end. Concluding once again that the capillary forces are really large.

Experiments were done trying to lift added structures to the normal folding structure. It was no problem to lift this added structure from the plane. We made a micro billboard for "University Twente" and lifted this out of the plane. This opens new opportunities we could try create more elaborate self-assembling structures which work on this principle.

6.1 RECOMMENDATION

There are still some unanswered questions. Like what is the substance that is left on the seam, which is keeping the structure from folding back. We have to analyze this substance to get a clear idea of the forces that are keeping these structures from folding back. It is probable that more than just the glue is keeping the flaps together. Folding experiments without this substance need to be performed to determine whether there are any other forces keeping these structure together. One can think of electrostatic forces, hydrogen bonds or van der Waals interaction.

We have to consider new ways of delivering water droplets to the structure. Positioning a fiber from the top for every single template is not a good method for mass production. We could consider delivering water through a nozzle like that of an inkjet printer. Or delivering water from the bottom of the structure through a channel in the middle of the structure. For this last solution the group has already made some samples to do initial experiments. Figure 48 and Figure 49 are SEM photos showing the structures from different angles.

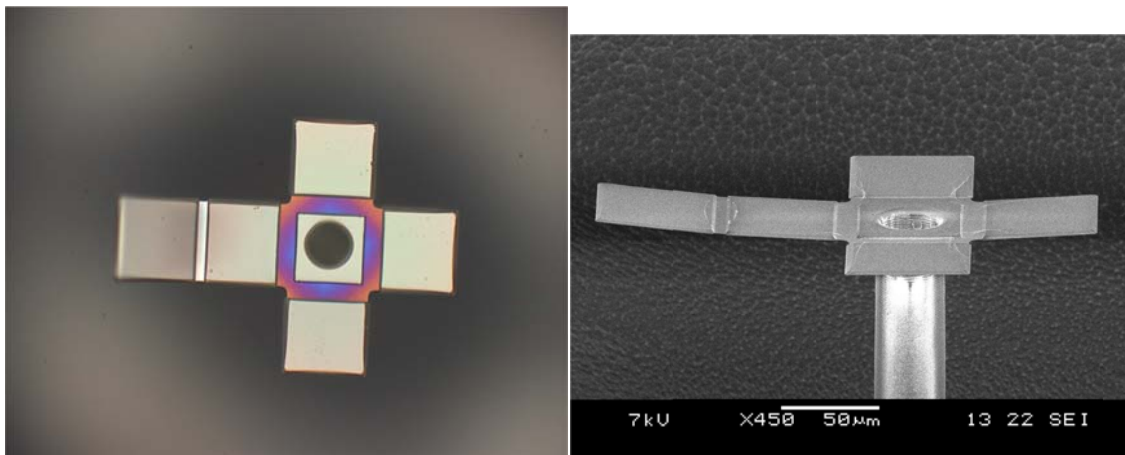


FIGURE 47 TEMPLATE OF A CUBE WITH A CHANNEL (TOPVIEW LEFT OPTICAL MICROSCOPE, SIDE VIEW ELECTRON MICROSCOPE)

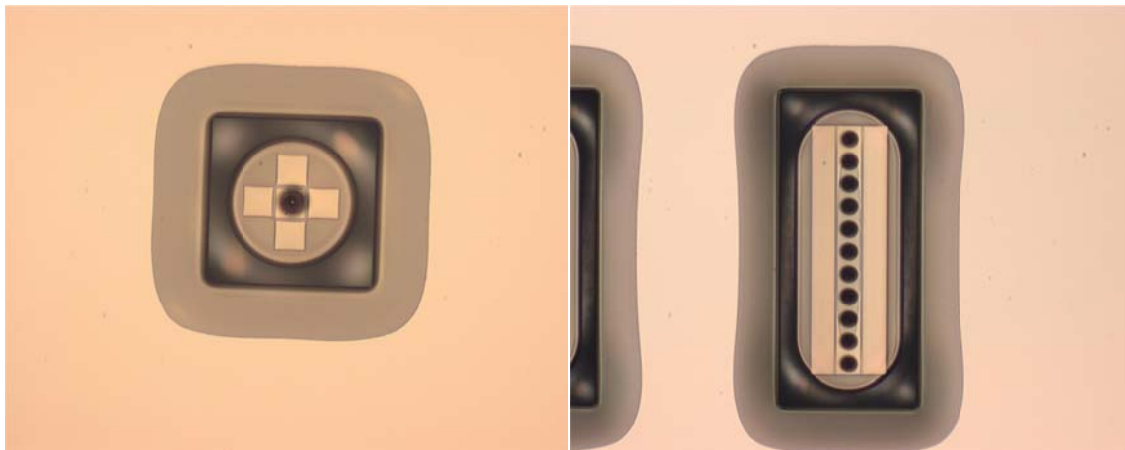


FIGURE 48 TOPVIEW OF STRUCTURES WITH CHANNELS

Close up images made by a SEM show us the ridges created by this process is shown in Figure 49. The holes created have a diameter of $34\mu\text{m}$. Initial experiments by holding this structure upside down and putting a drop of water on the channel did not result in the water flowing through the channel. The pressure is too large for the drop of water to get through the channel, a suggestion would be to create a column of water on the channel so that gravity will generate enough pressure to get the water through the channels.

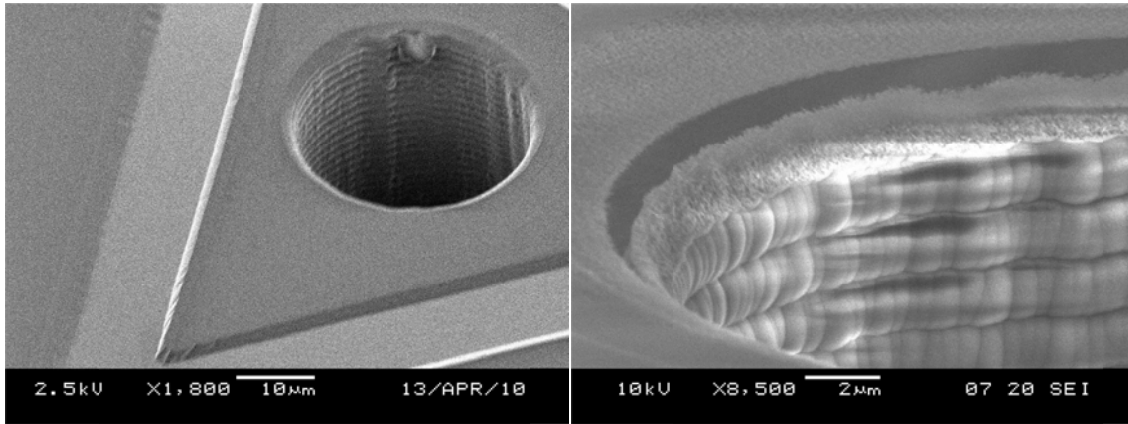


FIGURE 49 CHANNEL

7 BIBLIOGRAPHY

1. www.mems.sandia.gov, Sandia National Laboratories SUMMIT(TM) Technologies.
2. *Capillary Origami: Spontaneous Wrapping of a Droplet with an Elastic Sheet*. **Charlotte Py, Paul Reverdy, Lionel Doppler, José Bico, Benoît Roman, and Charles N. Baroud**. 156103, s.l. : Physical Review Letters, 2007.
3. *MEMS*. **R.R.A. Syms, E.M. Yeatman, V.M. Bright, and G.M. Whitesides**. 12,4, 2003.
4. *Elastocapillary fabrication of three-dimensional microstructures*. **J. W. van Honschoten, J. W. Berenschot, T. Ondarçuhu, R. G. P. Sanders, J. Sundaram, M. Elwenspoek, and N. R. Tas**. 97, 2010, APPLIED PHYSICS LETTERS.
5. *Applications of fluorocarbon polymers in micromechanics and micromachining*. **Jansen, H.V., et al., et al.** 1994, Sensors and Actuators, Vol. 1994, pp. 136-140.
6. *Casimir and van der Waals forces between two plates or a sphere lens above a plate made of real metals*. **G. L. Klimchitskaya, U. Mohideen and V. M. Mostepanenko**. 2000, PHYSICAL REVIEW A.
7. *MATERIALS ANALYSIS OF FLUOROCARBON FILMS*. **J. Elders, H. V. Jansert and M. Elwenspoek**.
8. *Surface Tension-Powered Self-Assembly of Microstructures—The State-of-the-Art*. **Richard R. A. Syms, Eric M. Yeatman, Victor M. Bright and George M. Whitesides**. Vol. 12 No. 4, s.l. : Journal of Microelectromechanical systems, 2003.
9. **Pierre-Gille de Gennes, Façoise Brochard-Wyart**. *Capillarity and Wetting Phenomena*. Paris : Springer Science+Business Media, Inc., 2003.
10. *Critical Review: Adhesion in surface micromechanical structures*. **Maboudian, Roya and Howe, Roger T.** 15, s.l. : American Vacuum Society, 1997. S0734-211X(97)02301-9.

8 APPENDIX – PROCESS DOCUMENTS

Capillary origami. Approach 3.

Silicon nitride structure on a silicon support with flap deviations

1. Introduction
 - 1.1 Design description
 - 1.2 Explanation of typical process steps
 - 1.3 Masks
2. Mask layout (overview)
3. Process outline wafer
4. Specific design parameters
5. Procesparameters
 - 5.1 Wafer selection
 - 5.2 Top wafer processing
 - 5.3 Bottom wafer processing
 - 5.4 Anodic bonding
6. Processdata form

1 Introduction

1.1 Design description

This structure is developed on the structure defined in the process document of J.W. van Honschoten.

The flaps in these structures are shaped differently to assess different aspects of folding. There are five different type of structures. One type of structure will test torsion. When the flaps fold, they tend to fold seamlessly. So this structure is made of flaps that decrease in width over the length. You can see this in Figure 1 where the width D1 is larger than D2. When these flaps fold there might be torsion in the hinges. Question is whether these flaps will close seamlessly and overcome this toroidal force or will there be a seam. If they would close seamlessly then the hinge on one end of the structure will be stretched out while the hinge on the other end will be relatively relaxed.

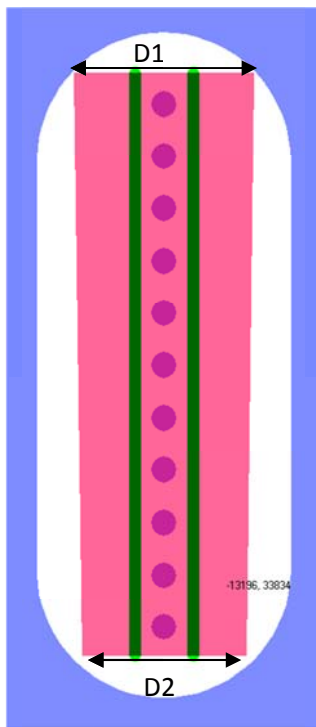
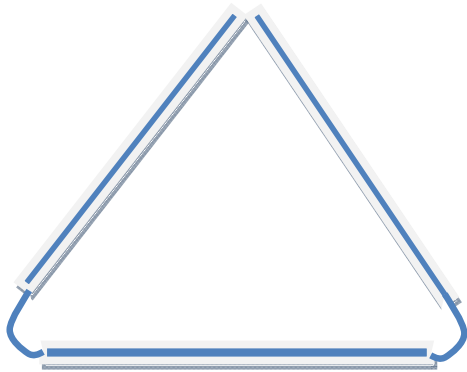
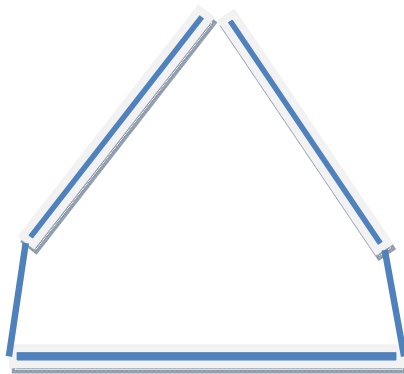


Figure 1 structure with decreasing flap widths



Rear view



Front view

Figure 2 distortion of the hinges

Next type of structures have flaps of different width, the left flap will have a smaller width than the right one as shown in Figure 3, the width D_2 is larger than D_1 . Again we will test whether these flaps will fold seamlessly. And if they do they can fold in two ways, the ends of the flaps meet each other, or one end of the flap will meet halfway of the other flap as shown in Figure 4. In the first case both the angles of the flaps will be the same, in the second case the angles will be different, ϕ_1 is not equal to ϕ_2 .

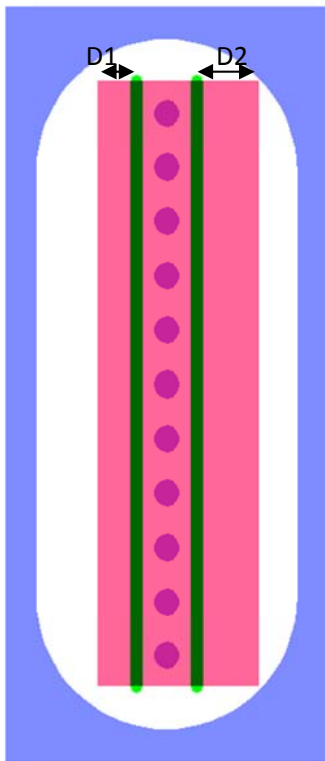


Figure 3 structure with different flap widths

Third type of structures will have a varying contact surface. Previous experiments have shown that folded structures tend to stay folded despite of the elastic forces in the hinges. To test this phenomena we will vary the contact surface of the flaps and we will vary the elasticity of the hinges to see what kind of effect these variables have.

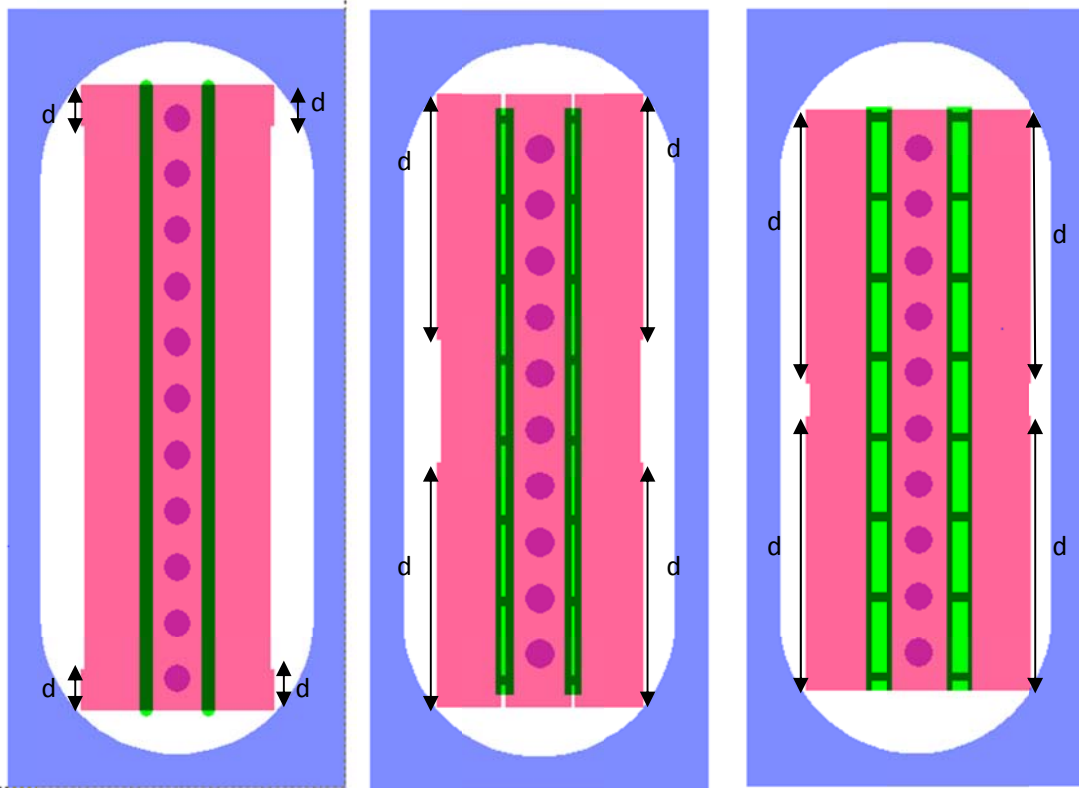


Figure 5 structure with varying contact surface

The edges of the flaps make contact really well due to the 45 degrees slope on the edges of the flaps (Figure 6 a). This is beneficial for the adhesive properties of these structures. Once they are folded the stay folded. To test how this property varies we devised a structure with flexible edges as shown in Figure 6 b and Figure 7. The edges have to be at least $5\mu\text{m}$ in width due to overcome unalignment and errors in processing. Smaller form factors will not be produced properly.

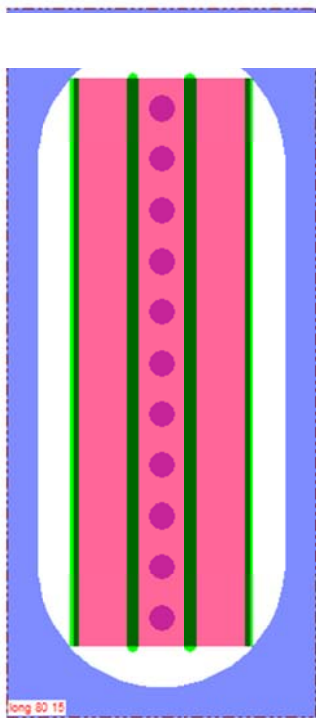


Figure 7 structures with flexible edges

Last but not least we will try to lift a structure of the surface using this folding action. For this experiment we created structures with the letters of the university on the flaps. When the flaps fold these letters will be lifted from the plane and we will have a micro billboard. In the same time that the flaps are under etched the letters will be etched free from the underlying silicon, and thus hang freely like the flaps.

This design has a small hole in the 'arm' that is holding the letter. This hole is made for the under etching to perform well. The addition to the structure which holds the letter can cause the under etching not to free the right flap from the center flap as shown in Figure 9. The hole will make it possible for the etchant to reach in the center of the arm.

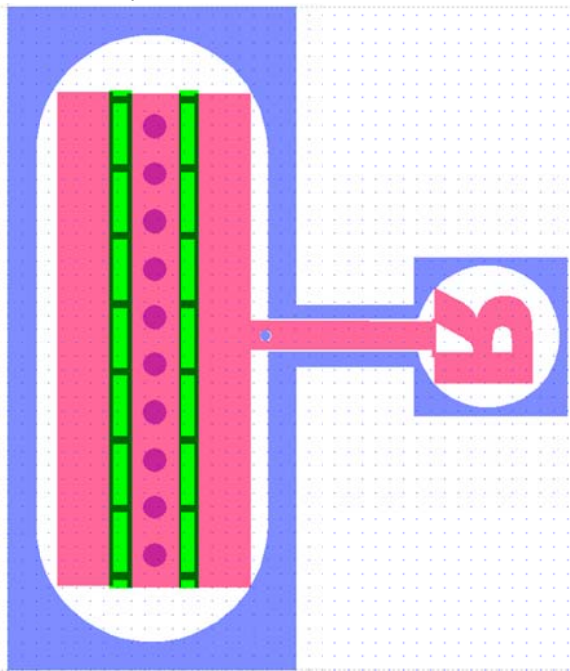


Figure 8 structure with a letter

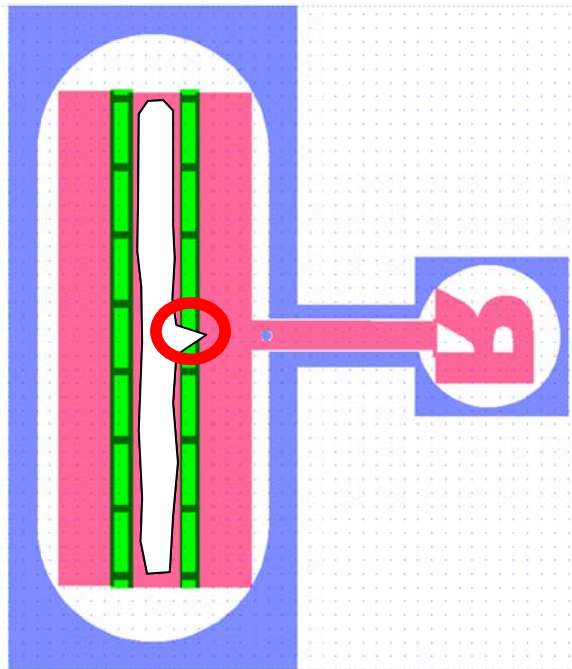


Figure 9 where it can go wrong with underetching

1.2 Explanation of typical process steps

In step 20, plasma etching by (SF₆, Oxford) is chosen as process step for the underetching of the silicon wafer. This etching technique does not affect the silicon nitride structure. We are able to prevent stiction of the free standing structures by adhesion due to capillary forces, since the silicon is completely removed by the plasma underetch under the folding flaps.

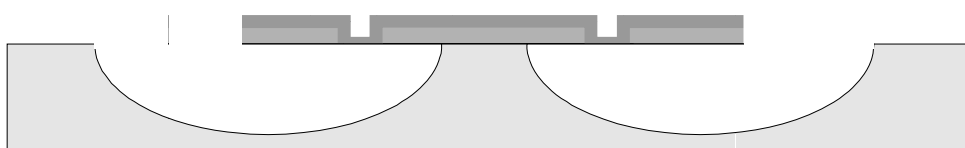
As already stated in the previous paragraph, when using the structure with the arm and letters, it is necessary to make a hole in the arm so that the under etching process won't get interrupted.

1.3 Masks

Example:

Three masks are needed:

- FOLD : Definition of folding locations.
- GEOM : Definition of final geometries of the structures
- UND: Definition of space in the silicon to be underetched



2 Mask layout (overview)

Filename: maskerCapOr_fluidchannelvJ3.cif

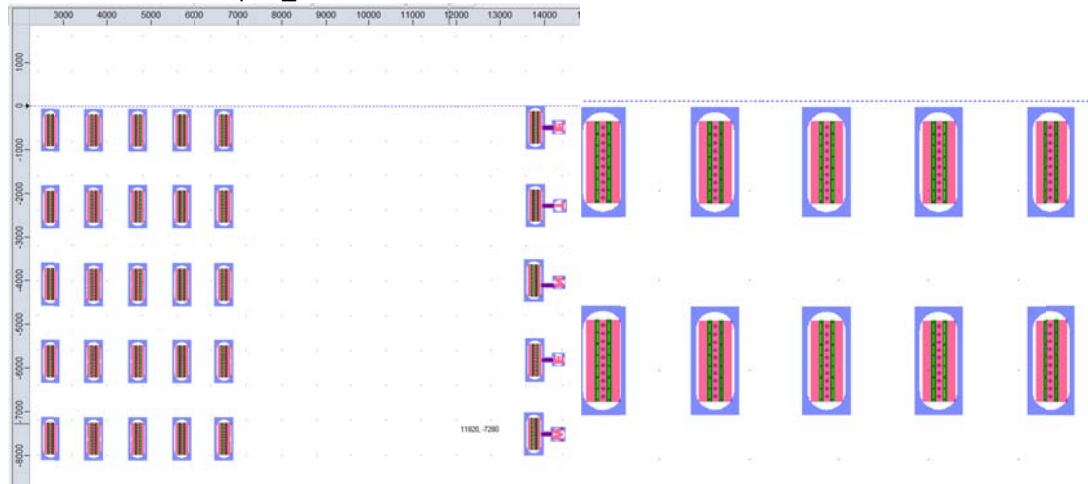
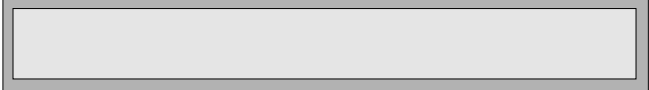
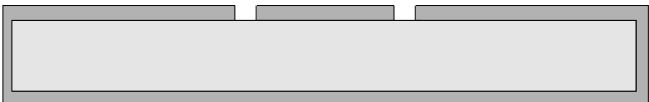
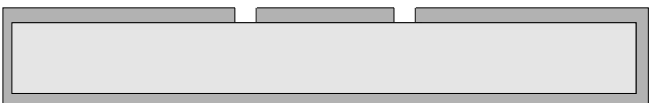
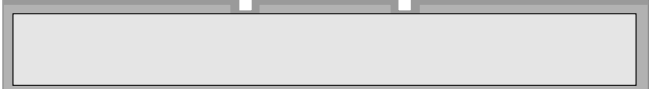
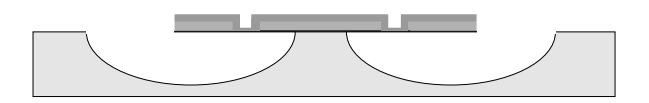
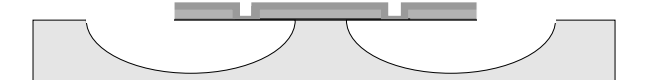


Figure above: part of the mask showing some of the structures (red = GEOM; green = FOLD; purple = UND)

| position | description | code | layer | inside white / black |
|----------|-----------------------------|------|-------|----------------------|
| | Definition of underetching | UND | | Inside white |
| | Outline of the geometries | GEOM | | Inside black |
| | Definition of folding lines | FOLD | | Inside white |

3 Process outline wafer

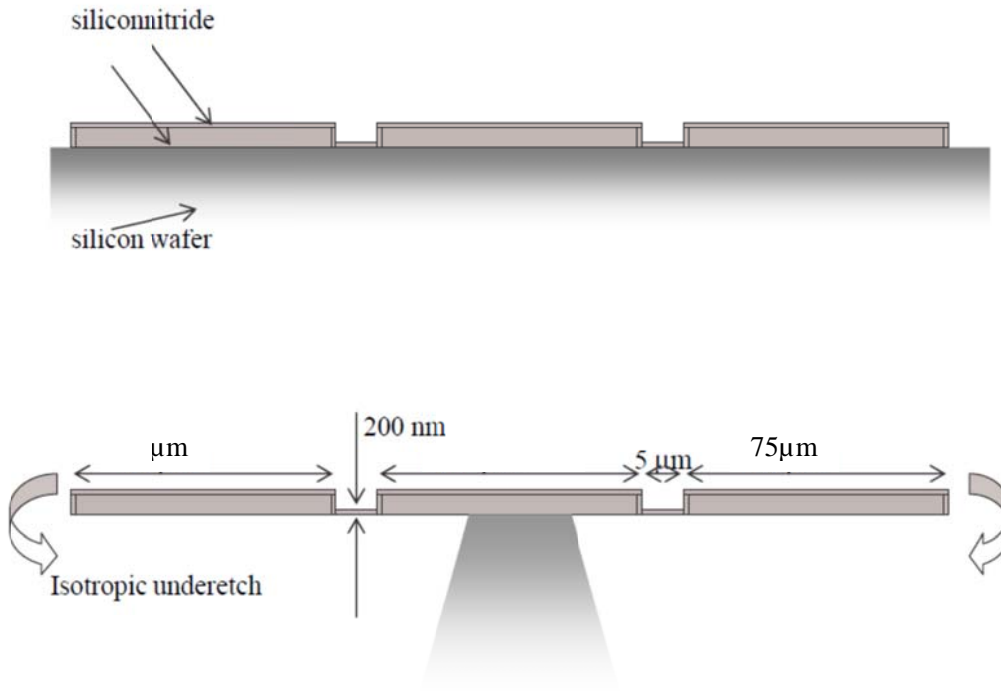
| Step | Process description | Cross-section after process |
|------|---|-----------------------------|
| 1. | Substrate selection - Silicon <100> OSP (#subs001) | |
| 2. | Cleaning Standard (#clean003) Etching HF (1%) user made (#etch028) | |

| | | |
|-----|--|--|
| 3. | LPCVD SiRN - low-depostion rate (#depo002) |  |
| 4. | Lithography - Olin 907-17 (#lith057) Lithography - Postbake standard (#lith009) Plasma etching SiN (Etske) (#etch004) |  |
| 5. | Stripping of Olin PR by oxygen plasma Tepla 300E (#lith017) Cleaning Standard (#clean003) Etching HF (1%) user made (#etch028) |  |
| 6. | LPCVD SiRN - low-depostion rate (#depo002) |  |
| 7. | Lithography - Olin 907-17 (#lith057) Lithography - Postbake standard (#lith009) Plasma etching SiN (Etske) (#Etch 072) |  |
| 8. | Stripping of Olin PR by oxygen plasma Tepla 300E (#lith017) Cleaning Standard (#clean003) |  |
| 9. | Lithography - Olin 907-17 (#lith057) Lithography - Postbake standard (#lith009) Etching HF (1%) user made (#etch028) Plasma etching of Silicon - standard (Oxford) (#etch013) |  |
| 10. | Stripping of Olin PR by oxygen plasma Tepla 300E (#lith017) |  |

Projectnr. : Number
Project : Project
Author : J.Sundaram

Revision : 01Page : 11 of 23
Rev. by : J.Sundaram : 2010-05-05
File : procesdocument approach 3.doc

4 Specific design parameters



5 Process parameters

Top wafer: p-type, <100> oriented, DSP

5.1 Wafer selection (only a top wafer)

| Step | Process | Process parameters | Design related parameters and Remarks |
|------|--|---|---------------------------------------|
| 1. | Substrate selection - Silicon <100> OSP (#subs001) | CR112B / Wafer Storage Cupboard Supplier: Orientation: <100> Diameter: 100mm Thickness: 525µm +/- 25µm Polished: Single side Resistivity: 5-10Ωcm Type: p | silicon wafer |
| 2. | Cleaning Standard (#clean003) | CR112B / Wet-Bench 131 HNO ₃ (100%) Selectipur: MERCK HNO ₃ (69%) VLSI: MERCK <ul style="list-style-type: none"> • Beaker 1: fuming HNO₃ (100%), 5min • Beaker 2: fuming HNO₃ (100%), 5min • Quick Dump Rinse <0.1µS • Beaker 3: boiling (95°C) HNO₃ (69%), 10min • Quick Dump Rinse <0.1µS • Spin drying | wet chemical cleaning of the wafer |
| 3. | Etching HF (1%) user made (#etch028) | CR116B / Wet-Bench 2 HF (1%) VLSI: MERCK 112629.500 <ul style="list-style-type: none"> • Quick Dump Rinse <0.1µS • Spin drying | |
| 4. | LPCVD SiRN - low-deposition rate (#depo002) | CR125C / Tempres LPCVD new system 2007 program: SiRN01/N2 Tube: G3 <ul style="list-style-type: none"> • Use 5-8 boat fillers in front and back of the boat to achieve specifications • SiH₂Cl₂ flow: 77.5 sccm • NH₃ flow: 20 sccm | Thickness SiRN: 1000 nm |

| | | | |
|----|--|--|-----------|
| | | <ul style="list-style-type: none"> • temperature: 820/850/870°C • pressure: 150 mTorr • deposition rate: ± 4 nm/min • N_f: ± 2.18 • Stress (range): 200-280 Mpa • Boat position 12: 200 MPa (centre of the boat) • Boat position 1: 280 MPa (front of the boat) • Uniformity/wafer: <2% • Uniformity over the boat: (20 wafers): < 8% | |
| 5. | Lithography - Olin 907-17 (#lith057) | <p>CR112B / Suss Micro Tech Spinner (Delta 20) Hotplate 120 °C:</p> <ul style="list-style-type: none"> • Dehydration bake (120°C): 5min <p>HexaMethylDiSilazane (HMDS):</p> <ul style="list-style-type: none"> • Spin program: 4 (4000rpm, 20sec) <p>Olin 907-17:</p> <ul style="list-style-type: none"> • Spin program: 4 (4000rpm, 20sec) <p>Hotplate 95 °C:</p> <ul style="list-style-type: none"> • Prebake (95°C): 90s <p>CR117B / EVG 620 Electronic Vision Group 620 Mask Aligner:</p> <ul style="list-style-type: none"> • Hg-lamp: 12 mW/cm² • Exposure Time: 4sec <p>CR112B / Wet-Bench 11 Hotplate 120°C (CR112B or CR117B):</p> <ul style="list-style-type: none"> • After Exposure Bake (120°C): 60sec <p>Developer OPD4262:</p> <ul style="list-style-type: none"> • Time: 30sec in Beaker 1 • Time: 15-30sec in Beaker 2 • Quick Dump Rinse <0.1μS • Spin drying | Mask FOLD |
| 6. | Lithography - Postbake standard (#lith009) | <p>CR112B / Hotplate 120°C</p> <ul style="list-style-type: none"> • Time: 30min | |
| 7. | Plasma etching SiN (Etske) (#etch004) | <p>CR102A / Elektrotech PF310/340 Dirty chamber Styros electrode</p> <ul style="list-style-type: none"> • Electrode temp.: 10°C • CHF₃ flow: 25sccm | |

| | | | |
|-----|---|--|--|
| | | <ul style="list-style-type: none"> • O₂ flow: 5sccm • pressure: 10mTorr • power: 75W <p>Etchrate SiN = 50nm/min (for V_{DC}=-460V) Etchrate SiN = 75 nm/min (for V_{DC} = -580V) Etchrate Olin resist = 95nm/min If DC-Bias < 375V apply chamber clean (#etch003)</p> | |
| 8. | Stripping of Olin PR by oxygen plasma Tepla 300E (#lith017) | CR102A / Tepla 300E Barrel Etcher (2.45 GHz) Multipurpose sytem <ul style="list-style-type: none"> • O₂ flow: 200sccm (50%) • Power: 500W • Pressure: 1.2 mbar • Time: 10 min for 1-3 wafers, 400 nm/min • Time: 20 min for 4-10 wafers • End point detection by visual inspection of the plasma color. • Blue color means still photoresist on the wafer, purple means clean. | |
| 9. | Cleaning Standard (#clean003) | CR112B / Wet-Bench 131 HNO ₃ (100%) Selectipur: MERCK HNO ₃ (69%) VLSI: MERCK <ul style="list-style-type: none"> • Beaker 1: fuming HNO₃ (100%), 5min • Beaker 2: fuming HNO₃ (100%), 5min • Quick Dump Rinse <0.1μS • Beaker 3: boiling (95°C) HNO₃ (69%), 10min • Quick Dump Rinse <0.1μS • Spin drying | |
| 10. | Etching HF (1%) user made (#etch028) | CR116B / Wet-Bench 2 HF (1%) VLSI: MERCK 112629.500 <ul style="list-style-type: none"> • Quick Dump Rinse <0.1μS • Spin drying | |
| 11. | LPCVD SiRN - low-deposition rate (#depo002) | CR125C / Tempress LPCVD new system 2007 program: SiRN01/N2 Tube: G3 <ul style="list-style-type: none"> • Use 5-8 boat fillers in front and back of the boat to achieve specifications • SiH₂Cl₂ flow: 77.5 sccm • NH₃ flow: 20 sccm | 200 nm thickness SiRN (to be varied for different wafers) Note: in the first run, the thickness was 100 nm |

| | | | |
|-----|--|--|-----------|
| | | <ul style="list-style-type: none"> • temperature: 820/850/870°C • pressure: 150 mTorr • deposition rate: ± 4 nm/min • N_f: ± 2.18 • Stress (range): 200-280 Mpa • Boat position 12: 200 MPa (centre of the boat) • Boat position 1: 280 MPa (front of the boat) • Uniformity/wafer: <2% • Uniformity over the boat: (20 wafers): < 8% | |
| 12. | Lithography - Olin 908-35 (#lith059) | <p>CR112B / Suss Micro Tech Spinner (Delta 20) Hotplate 120 °C:</p> <ul style="list-style-type: none"> • Dehydration bake (120°C): 5min <p>HexaMethylDiSilazane (HMDS):</p> <ul style="list-style-type: none"> • Spin program: 4 (4000rpm, 20sec) <p>Olin 908-35:</p> <ul style="list-style-type: none"> • Spin program: 4 (4000rpm, 20sec) <p>Hotplate 95 °C:</p> <ul style="list-style-type: none"> • Prebake (95°C): 120s <p>CR117B / EVG 620 Electronic Vision Group 620 Mask Aligner:</p> <ul style="list-style-type: none"> • Hg-lamp: 12 mW/cm² • Exposure Time: 9sec <p>CR112B / Wet-Bench 11 Hotplate 120°C (CR112B or CR117B):</p> <ul style="list-style-type: none"> • After Exposure Bake (120°C): 60sec <p>Developer OPD4262:</p> <ul style="list-style-type: none"> • Time: 30sec in Beaker 1 • Time: 15-30sec in Beaker 2 • Quick Dump Rinse <0.1μS • Spin drying | |
| 13. | Lithography - Postbake standard (#lith009) | <p>CR112B / Hotplate 120°C</p> <ul style="list-style-type: none"> • Time: 30min | |
| 14. | Plasma etching SiN (Etske) (#Etch 072) | <p>CR102/ Electrotech PF310/340</p> <p>Application: roughening of SiRN for Pt adhesion</p> <p>remarks: If Silicon surface is exposed to plasma us a short etch time</p> | Mask GEOM |

| | | | |
|-----|--|---|----------|
| | | <p>Sputter directly after etching step Pt layer (maximum delay time 10 min)</p> <p>Dirty chamber Styros electrode</p> <ul style="list-style-type: none"> • Electrode : 10 °C • SF₆: 30 sccm • O₂: 5 sccm • pressure: 40 mTorr • Power: 60 Watt • Time: 30 sec | |
| 15. | <p>Stripping of Olin PR by oxygen plasma Tepla 300E (#lith017)</p> | <p>CR102A / Tepla 300E Barrel Etcher (2.45 GHz) Multipurpose sytem</p> <ul style="list-style-type: none"> • O₂ flow: 200sccm (50%) • Power: 500W • Pressure: 1.2 mbar • Time: 10 min for 1-3 wafers, 400 nm/min • Time: 20 min for 4-10 wafers • End point detection by visual inspection of the plasma color. • Blue color means still photoresist on the wafer, purple means clean. | |
| 16. | <p>Cleaning Standard (#clean003)</p> | <p>CR112B / Wet-Bench 131 HNO₃ (100%) Selectipur: MERCK HNO₃ (69%) VLSI: MERCK</p> <ul style="list-style-type: none"> • Beaker 1: fuming HNO₃ (100%), 5min • Beaker 2: fuming HNO₃ (100%), 5min • Quick Dump Rinse <0.1μS • Beaker 3: boiling (95°C) HNO₃ (69%), 10min • Quick Dump Rinse <0.1μS • Spin drying | |
| 17. | <p>Lithography - Olin 908-35 (#lith059)</p> | <p>CR112B / Suss Micro Tech Spinner (Delta 20) Hotplate 120 °C:</p> <ul style="list-style-type: none"> • Dehydration bake (120°C): 5min <p>HexaMethylDiSilazane (HMDS):</p> <ul style="list-style-type: none"> • Spin program: 4 (4000rpm, 20sec) <p>Olin 908-35:</p> <ul style="list-style-type: none"> • Spin program: 4 (4000rpm, 20sec) <p>Hotplate 95 °C:</p> <ul style="list-style-type: none"> • Prebake (95°C): 120s <p>CR117B / EVG 620 Electronic Vision Group 620 Mask Aligner:</p> <ul style="list-style-type: none"> • Hg-lamp: 12 mW/cm² • Exposure Time: 9sec | Mask UND |

| | | | |
|-----|---|--|--|
| | | <p>CR112B / Wet-Bench 11 Hotplate 120°C (CR112B or CR117B):</p> <ul style="list-style-type: none"> • After Exposure Bake (120°C): 60sec <p>Developer OPD4262:</p> <ul style="list-style-type: none"> • Time: 30sec in Beaker 1 • Time: 15-30sec in Beaker 2 • Quick Dump Rinse <0.1µS • Spin drying | |
| 18. | Lithography - Postbake standard (#lith009) | <p>CR112B / Hotplate 120°C</p> <ul style="list-style-type: none"> • Time: 30min | |
| 19. | Plasma etching of Silicon - release (Oxford) (#etch070) | <p>CR102A / Oxford Plasmalab 100 ICP Application: release of membranes and cantilever SLE = poly-silicon</p> <ul style="list-style-type: none"> • Temp.: 20°C • SF₆ flow: 120sccm • CM pressure: 10mTorr • ICP power: 600W • He pressure: 20mbar <p>Cleaning step: Optional</p> <ul style="list-style-type: none"> • CCP power: 7.5W • V_{DC}: -40-55V • Time: 1min <p>SLE etching: xx min</p> <p>Etchrate SiRN: 5 nm/min</p> | <p>(Mask UND) Procedure of Isotropic etching step:</p> <p>take quarter piece. Use scotch tape to mount it on a 4" SiN wafer (thickness SiN ~ 1000nm)</p> <p>etchrate measured: Sample wafer 282 - Right-bottom t =60 min →48 micron underetch t=140 min →120 micron underetch → (RO_01) t=160 min →140 micron underetch → (RO_02) , this one is OK, so 140 micron</p> |
| 20. | Stripping of Olin PR by oxygen plasma Tepla 300E (#lith017) | <p>CR102A / Tepla 300E Barrel Etcher (2.45 GHz) Multipurpose sytem</p> <ul style="list-style-type: none"> • O₂ flow: 200sccm (50%) • Power: 500W • Pressure: 1.2 mbar • Time: 10 min for 1-3 wafers, 400 | |

| | | | |
|--|--|--|--|
| | | nm/min <ul style="list-style-type: none">• Time: 20 min for 4-10 wafers• End point detection by visual inspection of the plasma color.• Blue color means still photoresist on the wafer, purple means clean. | |
|--|--|--|--|

5.2 Wafer processing

The actual cooking of the wafer processing can be performed online using the TST Technology website, which can be found on:

<http://tst-server1/tst/>

**Remarks and results (Erwin):
(the required changes in the process document and in the mask have been made)**

-masks: 1) Put names on the masks (names have been added, JvH)
2) dimension of the hinges to critical for specific designs (changes have been made, JvH).
3) if we want to do the isotropic etching on waferscale → mask 3 should be uniform
4) now 2 times thick nitride etching → is it possible to do it in one run?
5) for metal hinges → design should be in such a way that there is only metal on places where the hinges are.

Process:

Step 11) thickness of the second SiN layer was ~ 100nm: see the note (JvH) in step 11
12) step coverage problem: next time we should use thicker resist (908-35) because of the large step in the SiN (1 micron)
17) see step 12) use 908-35
After step 18) is the usual HF etching not necessary because step 19) is started with a 1 min directional etch. (see opticonal cleaning step.)
19) Oxford system is used: see recipe below: #etch 070

Plasma etching of Silicon - release (Oxford) - CR102A / Oxford Plasmalab 100 ICP
Application: release of membranes and cantilever
(#etch070) SLE = poly-silicon

- Temp.: 20°C
- SF₆ flow: 120sccm
- CM pressure: 10mTorr
- ICP power: 600W
- He pressure: 20mbar

Cleaning step: Optional

- CCP power: 7.5W
- V_{DC}: -40-55V
- Time: 1min

SLE etching: xx min

Etchrate SiRN: 5 nm/min

For the isotropic dry etching of single crystalline silicon:

Maskmaterial:

Olin 908/35

Load: only a few % of the silicon is etched away

Procedure of Isotropic etching step:

- take quarter piece. Use scotch tape to mount it on a 4" SiN wafer (thickness SiN ~ 1000nm)
- etchrate measured: Sample wafer 282 - Right-bottom
 - t =60 min →48 micron underetch
 - t=140 min →120 micron underetch → (RO_01)
 - t=160 min →140 micron underetch → (RO_02) , this one is OK, so 140 micron underetch is needed to free the whole structure
- After 90 min of etching the photoresist is not shiny anymore: temperature problem!

This will cause not a serious problem. After stripping the resist the structures are shiny again, see picture below.

When we do this isotropic etching step on waferscale, the temperature will be constant due to good Helium backside contact and this problem will not occur.

Another option to avoid this effect when using quarter pieces: use fomblin oil to make a good thermal contact with the dummy wafer.

SEM images:

Overview of the mask: